How odd is Betelgeuse?

Martin O'Shaughnessy

Lund Observatory
Lund University

2020-EXA169

Degree project of 15 higher education credits
June 2020

Supervisor: Ross Church

Lund Observatory
Box 43
SE-221 00 Lund
Sweden

Abstract

The role of massive stars (those with masses greater than eight solar masses) in the chemical enrichment of galaxies and renewed star formation forms an important field of fundamental research in modern astrophysics. The complex nature of massive star evolution produces formidable challenges in furthering our understanding of the processes driving massive star evolution. Our ever-changing picture is further complicated by the relatively recent realisation that the vast majority of massive stars are formed in multiple star systems. In close binaries, interactions between the stars can lead to an exchange of matter, dramatically altering the structure and evolution of the component stars and the binary system as a whole. Depending on the initial binary configuration, this transfer of mass may be stable or unstable, producing results varying from wide binaries with massive secondaries, to common envelopes with tight binaries or even stellar mergers. A fraction of binary systems will be disrupted when the primary star explodes as a supernova, producing a runaway secondary star.

α-Orionis, commonly known as Betelgeuse, is believed to be the product of such a scenario. We synthesise a realistic population of binary systems containing massive stars and simulate the evolution of these systems accounting for mass transfer through Roche lobe overflow. We analyse the probability for each system to be disrupted after the supernova explosion of the primary for a range of supernova kicks and determine which fraction of these systems will produce a secondary star in the estimated mass range of Betelgeuse. We also investigate which mass transfer channel is most likely to produce a Betelgeuse-like star.

We find that $\sim 14\%$ and $\sim 25\%$ of binaries will produce a secondary in the mass ranges $13-18\ M_{\odot}$ and $11-20\ M_{\odot}$, respectively, allowing for the large uncertainties in determining the mass of Betelgeuse. Of these Betelgeuse candidates, approximately 75% emerge from systems following stable mass transfer.

We show the dependence of the fraction of bound systems on the magnitude and direction of the supernova kick velocity and the pre-supernova orbital elements of the binary. We establish the requirement for substantial supernova kicks in the disruption of close binaries and the generation of runaway velocities consistent with that of Betelgeuse. We also briefly discuss mechanisms other than post-supernova ejections which lead to runaway massive stars and how these might apply to Betelgeuse-like stars.

Populärvetenskaplig Beskrivning

Mellan hösten 2019 och våren 2020, fängslades både professionella och amatöra astronomer av de besynnerliga händelserna av Betelgeuse. Den särskiljande, lysande röda supergiant av *Orions axel*, vanligtvis den tionde ljusaste stjärnan på himlen, började dämpa sig dramatiskt. Detta fick många att spekulera om dess överhängande förstörelse i en kataklysmisk supernovaexplosion. Man tror nu att denna tillfälliga minskning av ljusstyrkan orsakades förmodligen av damm och gas från stjärnan som fördunklade vår vy, men till och med världens ledande astrofysiker är osäkra på de exakta fysiska processerna bakom sådana händelser. Man kan naturligtvis undra varför en väl studerad stjärna som Betelgeuse forblir ett mysterium.

Så kallade dvärgstjärnor, som vår sol, lever länge. Det finns många av dem och är därför väl förstådda. Samma sak kan dock inte sägas om massiva stjärnor som Betelgeuse. De lever snabbt och dör unga, deras livslängd mäts i miljoner år istället för miljarder - bara ett ögonblick på kosmologiska tidsskalor. Att komplicera frågor ytterligare, studier tyder på att de flesta massiva stjärnor inte bildas isolerat; snarare är de födda i system som innehåller två (eller fler) stjärnor. När dess stjärnor utvecklas och påverkar varandra, utbyter de material, som förändra deras struktur och ytterligare utveckling.

Ett möjligt resultat av dessa interaktioner i ett binärt system är utkastet av den mindre stjärnan efter att dess partner exploderar som en supernova. Betelgeuse verkar vara en ensam, flyktig stjärna, rusande genom rymden med stor hastighet, långt borta från födelseplatsen. Det är då mycket troligt att den var en gång del av ett binärt system som senare kastades ut av dess mer massiva partner.

I det här arbetet, simulerar vi en population av binära system som innehåller massiva stjärnor. Vi utforskar de olika typerna av interaktioner som dessa stjärnor genomgår med varandra medan de utvecklas. Efter den mer massiva stjärnan exploderar som en supernova, analyser vi vilken procentandel av systemen producerar en flyktig stjärna som liknar Betelgeuse och bestämmer vad vi kan säga, om något alls, om Betelgeuses evolutionshistoria.

Contents

Chapter 1

Introduction

Red supergiants (RSG) are among the largest known stars in the universe. They evolve from massive stars, up to about 40 $M_\odot$ (Heuvel 2017), as they exhaust their hydrogen fuel, evolve off the main sequence, and transition to the fusion of helium in their cores. The study of RSGs constitutes a rich body of only partially answered questions in astrophysics. For example, the long list of possible mechanisms to describe the often observed photometric and spectroscopic variability in RSGs is indicative of the uncertainties in our present understanding. Similarly, the evolution of RSGs in binaries is an important element in constraining expected gravitational wave signals, given the probabilities of RSGs as progenitors of colliding neutron stars (Levesque 2017). Understanding the RSG phase is critical then to expanding our knowledge of the physics governing massive star evolution.

α-Orionis, popularly known as Betelgeuse, is one of the closest and most studied red supergiants (Meynet et al. 2013). Despite these apparent advantages, we can say almost nothing about Betelgeuse's physical properties with absolute certainty, let alone its history and evolutionary path. Stellar evolution models estimate Betelgeuse's birth mass to be about 15 $M_\odot$ based on luminosity and temperature measurements, but estimates of its distance from Earth vary over tens of parsecs (van Loon 2013) making any solid statements impossible. Its true birth mass has been placed at anywhere between 10 $M_\odot$ and 20 $M_\odot$ (Meynet et al. 2013; Chatzopoulos et al. 2020).

What we do know is that Betelgeuse is a rapidly rotating RSG, a runaway star, far from any star forming region and moving through space with a velocity of $\sim$ 30 km/s (Harper et al. 2017). Extrapolating Betelgeuse's trajectory back to its place of origin has proved challenging, with some suggesting the Orion OB1a association, while others suggest a succession of dynamical kicks have altered its course (Chatzopoulos et al. (2020) and references therein).

Betelgeuse's fast rotation rate and a possible late ejection from its birth environment strongly suggests Betelgeuse was once the companion star of a more massive primary in a binary. When the primary exploded as a supernova, the kick velocity disrupted the system, ejecting Betelgeuse as a solitary, runaway star.

We pose the question, 'How odd is Betelgeuse?'. RSGs are rare and usually quite dis-

tant, making direct comparisons of the known physical properties especially challenging. In this work, we focus on Betelgeuse as a runaway star. Chapter 2 examines some fundamental aspects of massive star formation and single star evolution. Particular emphasise is given to the role of massive stars in the chemical enrichment of the universe and, consequently, their importance in furthering our understanding of the universe. Chapter 3 explores the basic orbital dynamics of binary systems from Kepler's laws. We also look at the role of mass loss from stellar winds on binary evolution. In chapter 4, we delve deeper into the physics of mass transfer via the process of Roche lobe overflow. We introduce the principles of stable and unstable mass transfer, assess the orbital evolution of the binary system during mass transfer and evaluate the state of the binary on completion of mass transfer. Chapter 5 establishes criteria for determining whether a binary system remains bound or otherwise after a supernova explosion.

Our ultimate goal is to understand the interactions in binary systems that produce secondary stars in Betelgeuse's estimated mass range and determine which fraction of those systems will be disrupted in the eventual supernova explosion of the primary. Can we say if Betelgeuse really is especially peculiar or merely a familiar example of a commonplace subset of massive runaway stars?

Chapter 2

Massive Star Formation and Evolution

The ultimate fate of massive stars, those with masses greater than eight solar masses, is most often a violent, cataclysmic supernova explosion. The role of massive stars in the chemical enrichment of galaxies through the synthesis and dispersal of heavy elements and the mechanical energy input into the interstellar medium through strong stellar winds and supernova explosions is crucial to star formation and mixing of the interstellar matter (Tan et al. 2014; Limongi 2017). Understandably, massive star formation and evolution forms a key area of fundamental research in astrophysics.

Our current understanding of massive star evolution is comparatively lacking relative to lower mass stars, such as our Sun. Massive stars are short-lived, burning through their main sequence phase in as little as 10^6 years. For stars more massive than 10 $M_\odot$ the lifetime is roughly proportional to $M^{-2.5}$ (Heuvel 2017). The resultant relative paucity of samples and the complex nature of massive star evolution necessarily introduce greater uncertainty in the stellar evolution models.

2.1 Initial Mass Function

Star formation is a continual process in stellar nurseries across the galaxy and beyond. Due to their short lifespans, the number of massive stars over time decreases. Their relative numbers are fewer still owing to the lower probability of massive star formation relative to lower mass stars (Prialnik 2009). To get a broader understanding of the prevalence of massive stars, much work has focused on the initial mass function (IMF) which quantifies the distribution of stellar masses in star-forming environments.

The most widely adopted power-law IMF for stars with mass $m \geq 0.5\ M_\odot$ is

$$\xi(m)dm \propto m^{-2.3} \tag{2.1}$$

where $\xi(m)dm$ is the number of single stars in the mass interval $(m, m+dm)$ (Kroupa 2001).

In theory, the IMF should vary with temperature and pressure in different star-forming regions. Higher temperature should produce on average higher stellar masses (Kroupa 2001); lower radiation pressure in low metallicity star forming environments should also lead to higher average masses by facilitating easier accretion of the gas (Kroupa, Weidner, et al. 2013). Some variability has been seen in the IMF, but is yet not fully understood nor satisfactorily explained (McKee and Tan 2002; Geha et al. 2013; Kroupa, Weidner, et al. 2013; Villaume et al. 2017).

Since the IMF differs from the present day mass function (PDMF), due to dynamical mixing in populations and different lifespans based on mass, it is an important tool for estimating the mass exchange between stars and their environment, as well as determining mass distribution in stellar populations, since mass is the primary factor driving stellar evolution (Prialnik 2009).

2.2 Single Star Evolution

Massive stars, like all stars, form in giant molecular clouds (GMCs). The fundamental question of whether massive star formation is simply a scaled-up version of low-mass star formation or follows from different physical processes is not quite decided (Bonnell and Bate 2005). Theoretical models of natal massive star formation pursue two lines of inquiry, core accretion and competitive accretion. In the former, gravitational forces and turbulence form clumps in the molecular gas, which begin to coalesce and collapse to form protostars. Models suggest the pre-stellar core function reflects the initial mass function well (Tan et al. 2014).

In the case of competitive accretion, gas is drawn chaotically from a wider region of the clump eventually forming a massive protostar surrounded by low mass protostars. (McKee and Tan 2002). Alternatively, collisions between protostars in dense stellar clusters may produce massive stars through mergers. Models by Moeckel and Clarke (2011) suggest the timescales required for rapid collisional growth would not reproduce the observed IMF at higher masses; consequently, collisions in star forming regions play a comparatively minor role in massive star formation (Tan et al. 2014).

Massive stars of spectral types O and B joining the zero-age-main-sequence (ZAMS) occupy the upper left portion of the theorist's Hertzsprung-Russell (HR) diagram ($\log T, \log L$). Upon exhaustion of hydrogen in the core, they move off the main sequence, expanding rapidly across the Hertzsprung gap (horizontally to the right on the HR diagram), before their steep rise along the Hayashi track on the red supergiant branch (RSGB) to the upper right portion of the HR-diagram (figure 2.1). Studies of stellar populations in star clusters reveal important aspects of stellar evolution, not least the age of the cluster and provide strong evidence of the shorter lifespans of massive stars. Since stars in such clusters are assumed to have formed at approximately the same time, this so-called turn-off point, where massive stars leave the main sequence, permits a robust estimate of the age of the cluster. Comparative studies between clusters of different ages then facilitates a careful analysis of the stellar evolutionary model and is in fact a cornerstone of massive star evolutionary theory (Karttunen

et al. 2017).

This standard model replicates observational studies well, where massive stars are seen to evolve in isolation. The picture is greatly complicated by the presence of a companion star in binary (or multiple) star systems. Indeed, many examples exist of massive stars whose observed characteristics cannot be explained by this simple, single star evolutionary theory. Likewise, progenitors of many supernovae must have experienced some external interactions during their lifetimes (Parker 2017; Limongi 2017).

The consensus is that the majority of massive stars are not formed in isolation; rather, they emerge in systems of two (or more) stars, with estimates for massive star binary fractions ranging from greater than 0.5 up to 1 (Sana et al. 2012; Harper et al. 2017). Stars in close binary systems will exchange mass at various points in their lifetime, the types of binary interactions producing vastly different outcomes in the subsequent evolution of the system and its component stars. These interactions are fundamental to the understanding of massive star evolution and the investigation of such interactions informs the body of this work.

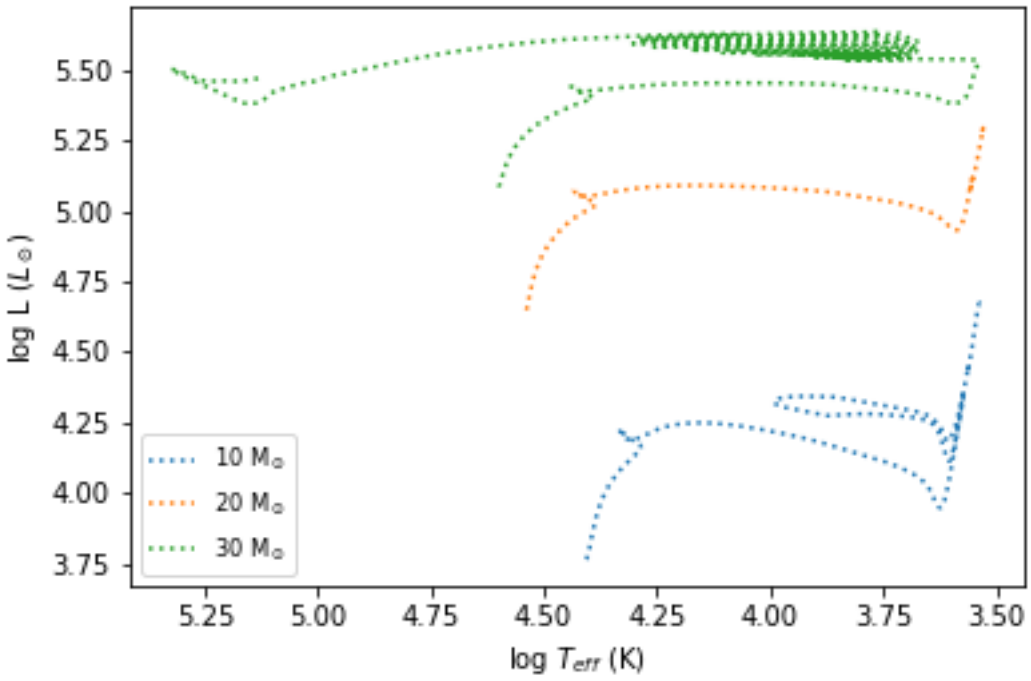

Figure 2.1: HR ($\log T$, $\log L$) tracks for massive stars with masses 10, 20, 30 $M_\odot$ (Church 2020)

Chapter 3

Binary Systems

3.1 Orbital Dynamics

We wish to understand what kind of interactions occur in binaries and how these affect the evolution of the binary components in contrast to single-star evolution. Most binaries from by fragmentation of protostellar cores or circumstellar discs (Tokovinin and Moe 2020). Observations of binary systems suggest a thermal eccentricity distribution for orbital periods $P \gtrsim 10^3$ days, where the population of binary systems have had sufficient time to reach a Boltzmann energy distribution, and $dN/de \approx 2e$. For $P \lesssim 10^3$, the eccentricity, $e \propto P$. (Kroupa and Burkert 2001). The minimum energy state in a binary system arises when orbital and spin angular momenta are aligned (Hut 1980). Furthermore, tidal interactions tend to circularise the orbits on timescales shorter than the nuclear timescale of main sequence H burning (Hurley, Tout, and Pols. 2002), in particular in close binaries (Pols 2011). For simplicity, we will thus focus our attention on binaries with circular orbits and corotating stars at time $t = 0$, even for systems with periods $P \gtrsim 10^3$ days.

In this scenario, the nature of the binary interaction is largely determined by the initial orbital period and mass ratio. For the two-body system in figure 3.1 with masses, m_1 and m_2, separated by a distance $r = r_1 + r_2$, the bodies orbit their common centre-of-mass, the barycentre. It follows that $r_1 m_1 = r_2 m_2$, where $r_{1,2}$ are the distances from the respective body to the centre-of-mass (CM). Alternatively, it can be shown that the distance $r_1 = \frac{m_2 r}{M}$, where M is the total mass of the system $m_1 + m_2$. From Kepler's third law the period P is then given by

$$\boxed{P = \left(\frac{4\pi^2}{GM} a^3\right)^{1/2}} \tag{3.1}$$

where the separation (semi-major axis) has been re-labelled with the more conventional a. For circular orbits the orbital velocity of star 1 is

$$v_1 = \frac{2\pi r_1}{P} \tag{3.2}$$

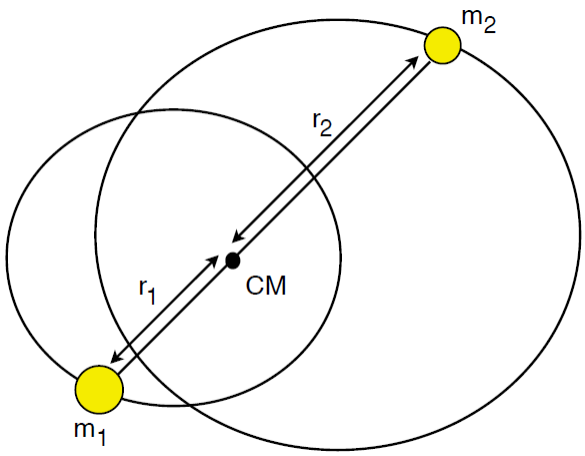

Figure 3.1: Binary System with masses $m_1 > m_2$. The centre-of-mass (CM) lies closer to the more massive star such that $m_1 r_1 = m_2 r_2$, i.e. $r_1 < r_2$.

and similarly for the companion star 2. We define the mass ratio q between the two stars as $q = m_1/m_2$, from which it follows

$$q = \frac{m_1}{m_2} = \frac{r_2}{r_1} = \frac{v_2}{v_1} \tag{3.3}$$

The angular momentum, J is given by

$$J = m_1 r_1 v_1 + m_2 r_2 v_2 \tag{3.4}$$
$$= (m_1 r_1^2 + m_2 r_2^2)\omega \tag{3.5}$$
$$= \left(\frac{m_1 m_2^2}{M^2} + \frac{m_2 m_1^2}{M^2}\right) a^2 \omega \tag{3.6}$$
$$= \frac{m_1 m_2}{M} a^2 \omega \tag{3.7}$$
$$\implies \boxed{J = \frac{m_1 m_2}{M}\sqrt{GMa}} \tag{3.8}$$

where ω is the angular velocity, M is the total mass, and we have used $\omega = 2\pi/P$ and Kepler's law (equation 3.1). From these apparently simple celestial mechanics, much can be inferred from the study of binaries, depending on which of the variables are known. Studies of eclipsing binaries, for example, allow us to determine masses and radii of stars, and have been crucial to furthering our understanding of processes in both binaries and individual stars.

3.2 Mass Loss

Mass loss is a feature of all stars but is of particular importance in the evolution of massive stars, including during the main-sequence phase (Prialnik 2009). Since stellar mass is

the prime factor in determining an individual star's evolution, high rates of mass loss can dramatically alter the fate of massive stars. For some massive stars, these stellar winds can be so powerful that they strip the star of its entire envelope leaving behind a bare hydrogen depleted core, so-called Wolf-Rayet stars (Smith 2014; Chiosi and Maeder 1986). Understanding the role of mass loss in massive stars is also important in establishing the progenitors of various supernova types. Together with examination of the post-SN circumstellar material, the pre-SN mass provides clues to the characteristics of the progenitor (Vink 2017). Determining the ZAMS stellar mass and subsequent pre-SN evolution depends crucially on the amount of mass lost in the star's life cycle. In interacting binary systems, this is especially complicated due to the complexities of mass transfer, the subject of the next section. First, we focus on mass loss from stellar winds before the onset of mass transfer.

In a binary system, the stellar wind carries off specific angular momentum of the mass-losing star

$$j_1 = \frac{J_1}{m_1} = r_1^2\omega = \left(\frac{m_2}{M}\right)^2 a^2\omega = \left(\frac{m_2}{M}\right)^2 \sqrt{GMa}$$

If star 1 loses mass at a rate $\dot{m}_1$, we have

$$\begin{aligned}
\dot{J} &= \dot{m}_1 j_1 = \dot{m}_1 \left(\frac{m_2}{M}\right)^2 \sqrt{GMa} \\
\implies \frac{\dot{J}}{J} &= \frac{\dot{m}_1 \left(\frac{m_2}{M}\right)^2 \sqrt{GMa}}{\frac{m_1 m_2}{M}\sqrt{GMa}} \\
&= \frac{m_2}{m_1}\frac{\dot{m}_1}{M} \\
&= \frac{\dot{m}_1}{m_1} - \frac{1}{2}\frac{\dot{m}_1}{M} + \frac{1}{2}\frac{\dot{a}}{a} \\
\implies \frac{1}{2}\frac{\dot{a}}{a} &= \frac{\dot{m}_1}{M}\left(\frac{m_2}{m_1} - \frac{m_1+m_2}{m_1} + \frac{1}{2}\right) \\
\implies \frac{\dot{m}_1}{M} &= -\frac{\dot{a}}{a} \\
\implies \frac{\mathrm{d}}{\mathrm{d}t}(\log M) &= -\frac{\mathrm{d}}{\mathrm{d}t}(\log a) \\
\implies \log M + \log a &= \text{const} \\
\implies \boxed{aM = \text{const}}
\end{aligned}$$

The product of the semi major axis and the total mass of the system is constant. Clearly if the primary loses mass, the separation a must increase.

In the next section, we discuss mass transfer via Roche lobe overflow (RLOF), but we briefly illustrate the significant effect mass loss through stellar winds can have on the evolution of a binary. Figure 3.2 shows the mass loss in a primary with initial mass $M_1 = 30\ M_\odot$ and subsequent widening of the orbit prior to filling its Roche lobe (here, the secondary has mass $M_2 = 10\ M_\odot$ and the initial separation is 2000 $R_\odot$). The 30 $M_\odot$ star experiences significant mass loss from stellar winds. The expansion of the orbit delays the onset of RLOF, which

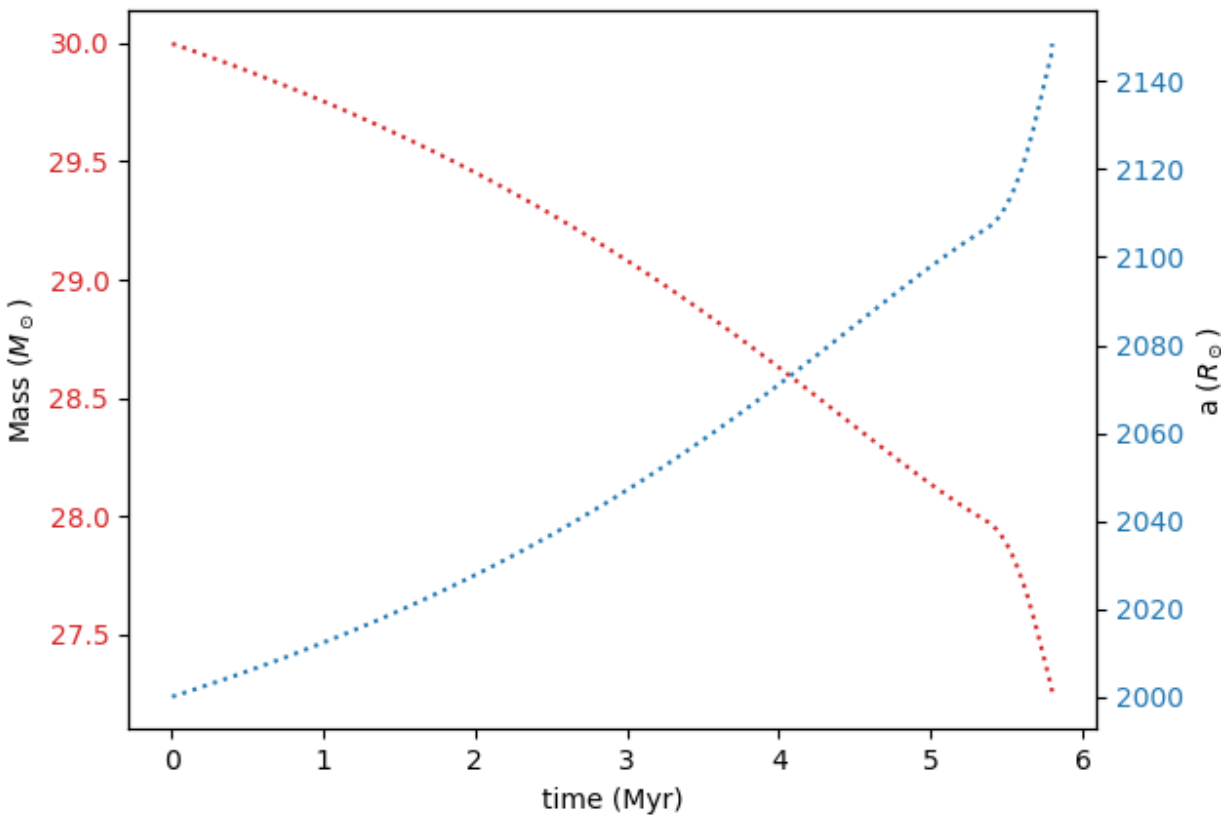

Figure 3.2: Significant mass loss from stellar winds in a primary with mass $M_1 = 30\ M_\odot$ (red) and subsequent orbital expansion (blue) of binary prior to the onset of mass transfer. Here, the secondary has mass $M_2 = 10\ M_\odot$ and the initial separation is 2000 $R_\odot$

can significantly alter the type of mass transfer. For example, RLOF could commence after the primary has reached the RSG branch instead of on the Hertzsprung gap. The reduction in mass may also lead to a reversal in the mass ratio by the time the primary fills its Roche lobe. In a wide binary, RLOF may not even occur at all due to the expanding orbit.

Chapter 4

Mass Transfer

There are essentially two mechanisms leading to mass transfer in binaries: if one of the stars ejects mass in a stellar wind, the companion star may accrete some of this matter; or, the companion may capture matter from the envelope of the primary through Roche lobe overflow. Only the most massive stars have stellar winds strong enough to greatly affect the evolution of the smaller companion (Nelson and Eggleton 2001; Neustroev 2017). We, therefore, focus our attention on mass transfer via Roche lobe overflow.

4.1 Roche Geometry

Consider a binary system with the origin at the primary. In cartesian coordinates (x, y, z), we define the x-axis joining the centres of the stars, the y-axis in the direction of orbital motion of the primary and the z-axis perpendicular to the orbital plane. Approximating the gravitational field generated by the stars as that of two point masses, the total potential, the Roche potential Φ_R is given by

$$\Phi_R = -\frac{GM_1}{\sqrt{x^2+y^2+z^2}} - \frac{GM_2}{\sqrt{(x-a)^2+y^2+z^2}} - \frac{1}{2}\Omega_{orb}^2\left[(x-\mu a)^2+y^2\right] \tag{4.1}$$

where $\mu = M_2/(M_1+M_2)$ and the orbital angular velocity $\Omega_{orb} = 2\pi/P_{orb}$. It can be shown that the Roche equipotentials are functions only of the mass ratio, q, their scales determined by a. Close to the centre of each star, the gravitational potential dominates and the equipotentials are approximately spherical and concentric. Farther from the stars, tidal effects produce elongation of the potential surfaces towards the companion star. The 3D potential surfaces are also flattened by centrifugal forces. Where the equipotentials meet, the forces between the two stars cancel (figures 4.1 and 4.2). The innermost equipotential surface which encloses both stars defines the Roche lobe of each star, within which material is gravitationally bound to the star (Neustroev 2017; Hurley, Tout, and Pols. 2002). If one star fills its Roche lobe, matter flows through the Lagrangian L_1 point and may be captured by the companion, in a process known as Roche lobe overflow (RLOF) (Eldridge 2017)

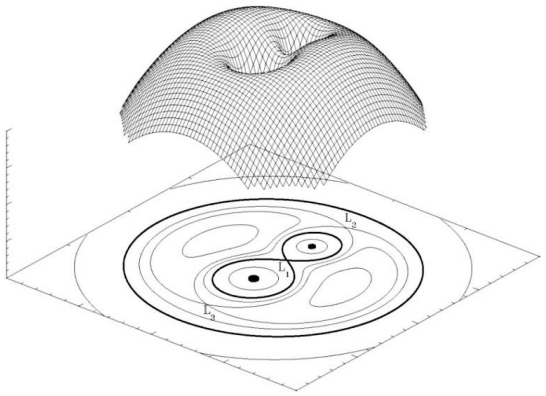

Figure 4.1: 3D representation of the Roche surface.

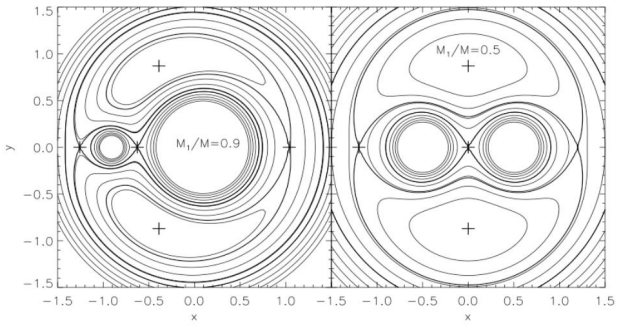

Figure 4.2: Contour plot of Roche lobes for mass ratios of 9 and 1 respectively. *Credit: Neustroev, University of Oulu.*

4.1.1 Roche Lobe Overflow

The Roche lobe radius, R_L, is the equivalent radius of the sphere of the volume $V = \frac{4}{3}\pi R_L^3$ defining the Roche lobe. A fitting formula derived by Eggleton (1983) has proven to be accurate to within 1% over the complete range of mass ratios (D. A. Leahy and J. C. Leahy 2015) with

$$\frac{R_L}{a} \approx \frac{0.49q^{2/3}}{0.6q^{2/3} + \ln\left(1 + q^{1/3}\right)} \tag{4.2}$$

Hydrostatic equilibrium in the corotating frame requires that the stellar surface coincides with an equipotential surface (Pols 2011) leading to three possibilities (figure 4.3):

- **Detached Binary:** both stars fill equipotential surfaces inside their respective Roche lobe. Their evolution, unaffected by Roche geometry, proceeds effectively as single-star evolution.
- **Semi-detached Binary:** one star fills its Roche lobe. Hydrostatic equilibrium is lost near the L_1 point and matter flows through the L_1 point.
- **Contact Binary:** both stars fill their Roche lobe at the L_1 point. The stars exchange both heat and mass.

In general, systems are formed as detached binaries. The expansion of the star(s) and/or angular momentum loss leads to orbital shrinking which, in close binaries, produces a semi-detached or contact binary. During the main-sequence, the radius increases by only a small fraction. For massive stars, rapid expansion across the Hertzsprung gap is followed by He burning as a red supergiant. Here the radius continues to expand, albeit at a much reduced rate and scale. (As mentioned, more massive stars, $M \gtrsim 25M_\odot$, lose their H-rich envelopes from strong stellar winds before He ignition, producing Wolf-Rayet stars with smaller radii)

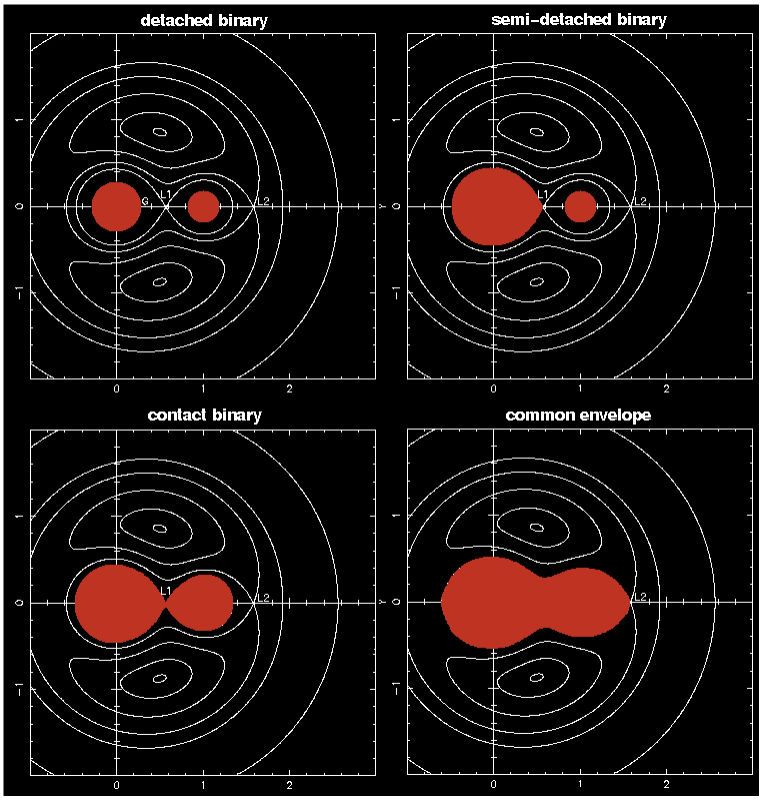

Figure 4.3: Possible binary configurations including CEE as discussed in the text. *Credit: Dhillon, University of Sheffield.*

It is instructive to distinguish three cases of mass transfer:

- **Case A:** The star fills its Roche lobe on the main sequence.
- **Case B:** The star fills its Roche lobe after core hydrogen burning is exhausted.
- **Case C:** The star expands after He exhaustion.

Which case of mass transfer ensues depends on the size of the Roche lobe R_L, the separation a and the mass ratio q. Also of crucial importance is the stability of mass transfer, largely determined by whether the donor has a radiative or convective envelope (discussed below). Figure 4.4 shows the change in radius of a 16 $M_\odot$ star from the ZAMS to the end of carbon burning. Also indicated are the approximate positions where mass transfer of types A, B or C are observed. The blue dashed line marks the boundary between where the star has a radiative envelope and a deep convective envelope as it becomes a red supergiant. Figure 4.5 illustrates the importance of the initial separation in determining at which stage of the primary's evolution RLOF occurs for given initial masses. The onset of mass transfer occurs at progressively later stages of the primary's evolution with increasing initial separation.

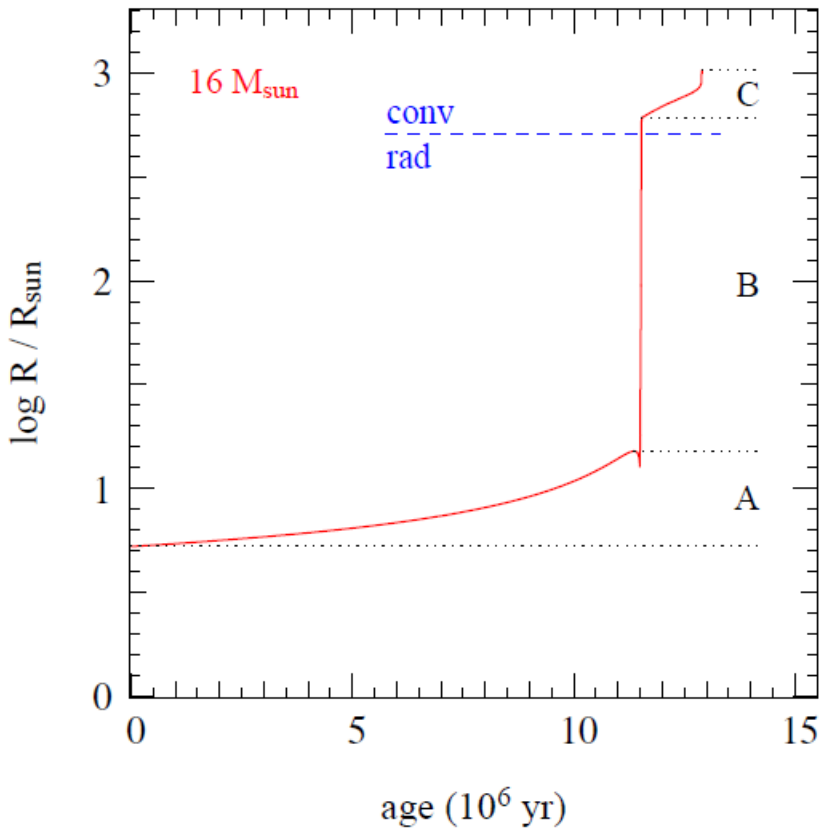

Figure 4.4: Change in radius of a 16 $M_\odot$ star from ZAMS to the end of carbon burning. *Credit: Pols, Utrecht University.*

4.2 Orbital Evolution During Mass Transfer

Since the orbital angular momentum is often much greater than the spin angular momentum of the stars, the total angular momentum, assuming a circular orbit, is approximately

$$J = \frac{M_1 M_2}{M}\sqrt{GMa} \tag{4.3}$$

where M is the total mass. In general, the orbital evolution is then determined by differentiating to give

$$2\frac{\dot{J}}{J} = \frac{\dot{a}}{a} + 2\frac{\dot{M}_1}{M_1} + 2\frac{\dot{M}_2}{M_2} - \frac{\dot{M}_1 + \dot{M}_2}{M_1 + M_2} \tag{4.4}$$

Conservative Mass Transfer

For conservative mass transfer, total mass and angular momentum are conserved such that $\dot{J} = 0$ and $\dot{M}_2 = -\dot{M}_1$ giving

$$\frac{\dot{a}}{a} = 2\left(\frac{M_1}{M_2} - 1\right)\frac{\dot{M}_1}{M_1} \tag{4.5}$$

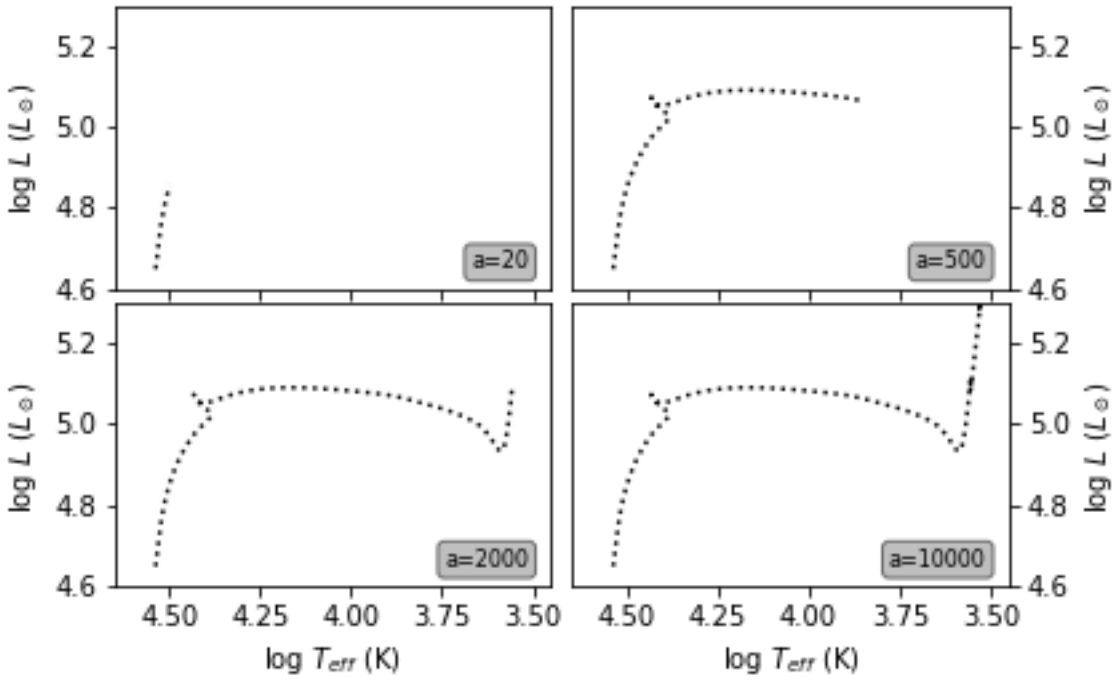

Figure 4.5: HR track of primary with mass $M_1 = 20\ M_\odot$ up to RLOF in a binary with secondary of mass $M_2 = 10\ M_\odot$. *Top Row:* With an initial separation of 20 $M_\odot$, the primary fills its Roche lobe on the main sequence (left); With $a = 500\ R_\odot$, RLOF begins across the Hertzsprung gap (right). *Bottom Row:* At $a = 2000\ R_\odot$, the primary is beginning its RSG phase (left); With an initial separation of 10,000 $R_\odot$, the primary never fills its Roche lobe and evolves as a single star.

Since $\dot{M}_1 < 0$, it follows that if $M_1 > M_2$, then $\dot{a} < 0$ and the orbit shrinks; if $M_1 < M_2$, then $\dot{a} > 0$ and the orbit expands. If the donor transfers an amount of mass ΔM to its companion, we have

$$\frac{M_1 M_2}{M}\sqrt{GMa_i} = \frac{(M_1 - \Delta M)(M_2 + \Delta M)}{M}\sqrt{GMa_f} \tag{4.6}$$

from which

$$a_f = a_i \left(\frac{M_1 M_2}{(M_1 - \Delta M)(M_2 + \Delta M)}\right)^2 \tag{4.7}$$

for the resultant semi-major axis a_f after mass transfer, where a_i is the initial separation.

Non-Conservative Mass Transfer

This simple formulation is complicated by mass loss and angular momentum loss leading to non-conservative mass transfer, a more realistic picture. In this case the companion accretes only a fraction of the matter flowing from the primary. Modelling the several modes of non-conservative mass transfer is notoriously complex (Soberman, Phinney, and van den Heuvel 1997) and we will assume that stable mass transfer is conservative.

4.2.1 Common Envelope Evolution

Dynamically unstable mass transfer in massive stars leads to common envelope evolution. The adiabatic response of the mass losing star is unable to prevent it overfilling its Roche lobe; the mass transfer rate increases and an unstable, runaway loss of mass from the primary ensues. The smaller companion is unable to accrete the ejected matter and a common envelope is formed, engulfing both stars.

Following the energy formulation of Tout et al. (1997), the total binding energy of the envelope is

$$E_{bind,i} = -\frac{GM_1M_{1,env}}{\lambda R_1} \tag{4.8}$$

where $M_{1,env}$ is the mass of the primary's envelope, λ depends on the structure of the donor's envelope, and R_1 is the radius of the envelope which for simplicity we set equal to a_i, the initial separation. The initial orbital energy of the system at the onset of RLOF is

$$E_{orb,i} = -\frac{1}{2}\frac{GM_{1,c}M_2}{a_i} \tag{4.9}$$

where $M_{1,c}$ is the mass of the primary's core. As the stars move through the expanding envelope, friction causes them to lose orbital momentum and the two stars spiral in, transferring orbital energy into the envelope with an efficiency parameter α. If we assume $\alpha = 1$, then the amount of energy transferred such that the entire envelope is ejected from the system can be expressed as

$$\Delta E = E_{orb,f} - E_{orb,i} = E_{bind,i} \tag{4.10}$$

with

$$E_{orb,f} = -\frac{1}{2}\frac{GM_{1,c}M_2}{a_f} \tag{4.11}$$

where a_f is the final separation and M_2 remains unchanged (i.e. we assume none of the ejected matter from the primary is accreted by the companion). The final separation is thus

$$a_f = a_i\left(\frac{M_{1,c}M_2}{2M_1M_{1,env} + \lambda M_{1,c}M_2}\right) \tag{4.12}$$

The final separation is smaller than the initial separation resulting in a tight binary or a stellar merger.

4.3 Stability of Mass Transfer

The stability criteria for the onset of mass transfer are the subject of much study (Hurley, Tout, and Pols. 2002). They are determined by the response of the donor radius to mass loss, the change in orbital separation and the response of the Roche lobe radius due to mass transfer. In practice, we compare the slopes of the mass-radius relation of the stellar radius

and Roche lobe radius, expressed as the mass-radius exponents (Soberman, Phinney, and van den Heuvel 1997), respectively

$$\zeta_* \equiv \frac{d\ln R_*}{d\ln M} \qquad \zeta_L \equiv \frac{d\ln R_L}{d\ln M} \tag{4.13}$$

If $\zeta_* \geq \zeta_L$, we have stable mass transfer, otherwise, unstable mass transfer. The picture is complicated by the readjustment of the star to mass loss on different timescales: the star attempts to recover hydrostatic equilibrium on its dynamical timescale but thermal adjustment is on the much slower Kelvin-Helmholtz timescale. The initial dynamical response of the stellar radius to mass loss is (almost) adiabatic with

$$\zeta_{ad} = \left(\frac{d\ln R_*}{d\ln M}\right)_{ad} \tag{4.14}$$

Dynamical stability of mass transfer is then governed by the condition $\zeta_{ad} \geq \zeta_L$. A thorough treatment of the various regimes can be found in Soberman, Phinney, and van den Heuvel (1997), Hurley, Tout, and Pols. (2002), and Pols (2011). For our purposes, we restrict our formulation to the structure of the envelope of the primary at the onset of mass transfer and the response of the Roche lobe radius to mass loss.

The Roche lobe radius depends mainly on the mass ratio, q. For conservative mass transfer, Soberman, Phinney, and van den Heuvel (1997) established a critical mass ratio as $\zeta_L = 2.13q - 1.67$ for $q < 10$. For stars with deep convective envelopes (RSG in our case), the star expands to maintain an approximately constant radius, with $\zeta_{ad} \leq 0$. Mass transfer is dynamically unstable unless mass loss due to stellar winds has reduced the mass of the initially more massive primary to $q \leq 5/6$ (Soberman, Phinney, and van den Heuvel 1997; Neustroev 2017) at the onset of RLOF.

If the star has a radiative envelope (case A or early case B for massive stars), then the star shrinks rapidly upon mass loss, as $\zeta_{ad} \gg 0$. Mass transfer is unstable only if the primary is much more massive than the companion. We adopt the critical mass ratio from Pols (2011) where we assume stable, conservative mass transfer for $q \leq 4$.

In this thesis, we assume stable mass transfer leads to conservative mass transfer and widening of the orbit. Additionally, all of the primary's envelope mass is received by the companion. Conversely, unstable mass transfer leads to non-conservative mass transfer and common envelope evolution (CEE) with orbital shrinking or mergers if $a_f < 1\ R_\odot$. In the case of an intact binary, we assume the companion's mass is unchanged in the common envelope (CE) phase. A summary of the stability criteria used in this paper is given in figure 6.3.

Chapter 5

Supernovae

Supernova (SN) explosions in binary systems occur on timescales much shorter than the orbital period (Postnov and Yungelson 2014) and one can assume that the mass lost is effectively instantaneous. In this approximation, the relative separation and the relative velocity remain effectively unchanged (Kulkarni 2010). Typically the supernova explosion is asymmetric and the remnant neutron star (or black hole) receives a kick velocity, $\mathbf{v_k}$.

Consider the pre-supernova binary system, with initial masses M_1 and M_2. The stars move in a circular orbit with initial separation a_i and relative velocity v, with $v = |\mathbf{v_1} - \mathbf{v_2}|$. The primary explodes as a supernova leaving behind a neutron star(NS) or black hole(BH) with mass M_c (Parker 2017).

Supernova without kick In the simple case where we assume there is no supernova kick, the explosion is symmetric in the primary's frame but not in centre-of-mass frame, leading to system recoil, *Blaauw–Boersma recoil* (Postnov and Yungelson 2014).

The equations of motion for 2 bodies (approximated as point masses) orbiting each other under the force of gravity is equivalent to a single body problem with mass μ moving in an external gravitational potential

$$\mu \frac{d^2\mathbf{r}}{dt^2} = -G\frac{M_1 M_2}{a^2} \tag{5.1}$$

with reduced mass $\mu = (M_1 M_2)/(M_1 + M_2)$. The total energy is then

$$E = \frac{1}{2}\mu v^2 - G\frac{M_1 M_2}{a} \tag{5.2}$$

From Kepler's 3rd law, it can be shown that

$$v^2 = G\frac{M_1 + M_2}{a}$$

When star 1 explodes as a supernova, it leaves behind a remnant neutron star of mass $M_c = 1.4\ M_\odot$. To re-iterate, the assumption of instantaneous mass loss assumes the relative separation, a, and relative velocity, v, are unchanged immediately after the SN explosion.

The sum of the kinetic energy and the gravitational binding energy of the post-explosion binary is then

$$E' = \frac{1}{2}\mu' v^2 - G\frac{M_c M_2}{a}$$

where $\mu' = \frac{M_c M_2}{M_c + M_2}$ is the reduced mass of the resulting system. Eliminating v^2, we get

$$E' = G\frac{M_c M_2}{2a}\left[\frac{M_1 + M_2}{M_c + M_2} - 2\right]$$

The post-SN orbit will be bound only if E' is negative. This occurs if and only if the mass lost in the explosion: $\Delta M < 1/2(M_1 + M_2)$.

Supernova with kick More generally, the supernova explosion is asymmetric and we need to account for the kick velocity in determining the state of the system post-supernova. For example, simulations have shown that modelling a 1% asymmetry in the neutrino momentum flux produces a kick velocity of order ~ 400 km/s (Brandt and Podsiadlowski 1994). In truth, much is unknown about the precise mechanisms governing asymmetry in supernovae explosions and is the subject of ongoing research. Our primary aim is to determine whether a binary system is disrupted following a supernova explosion. We outline an amalgamation of the work of Tout et al. (1997) and Brandt and Podsiadlowski (1994) in establishing the relevant criteria.

Consider a coordinate system where the x-axis is the line from M_1 to M_2, $\mathbf{v_i}$ is directed along the y-axis and the z-axis is perpendicular to the orbital plane. In this reference frame, the initial orbital velocity is $\mathbf{v_i} = (0, v_i, 0)$. The total orbital angular momentum is $\mathbf{J_i} = \mu_i a_i(0, 0, -v_i)$. Since we consider the explosion to be instantaneous the position of the exploding star is unchanged. However, with a kick velocity $\mathbf{v_k} = (v_{kx}, v_{ky}, v_{kz})$, the post-supernova relative velocity becomes $\mathbf{v_f} = (v_{kx}, v_i + v_{ky}, v_{kz})$ and the orbital momentum is now $\mathbf{J_f} = \mu_f a_i(0, v_{kz}, -(v_i + v_{ky}))$, where the reduced mass of the system is now $\mu_f = M_c M_2/(M_c + M_2)$. Equating both the total energy and absolute value of the orbital momentum of the initial system to those of the resulting elliptical system, respectively, gives

$$\frac{1}{2}\mu_f v_f^2 - \frac{GM_c M_2}{a_i} = -\frac{GM_c M_2}{2a_f} \tag{5.3}$$

and

$$\mu_f a_i \sqrt{v_{kz}^2 + (v_i + v_{ky})^2} = \mu_f \sqrt{G(M_c + M_2)a_f(1 - e^2)} \tag{5.4}$$

Solving for the resulting separation a_f gives

$$\frac{a_f}{a_i} = \left[2 - \chi\left(\frac{v_{kx}^2 + v_{kz}^2 + (v_i + v_{ky})^2}{v_i^2}\right)\right]^{-1} \tag{5.5}$$

The resulting eccentricity is then

$$1 - e^2 = \chi\frac{a_i}{a_f}\left(\frac{v_{kz}^2 + (v_i + v_{ky})^2}{v_i^2}\right) \tag{5.6}$$

where χ is the dimensionless mass relation $\chi \equiv (M_1 + M_2)/(M_c + M_2) = M/(M - \Delta M)$ The angle θ defines the change in direction between the orbital angular momentum pre- and post-supernova with

$$\cos\theta = \frac{\mathbf{J_i} \cdot \mathbf{J_f}}{|J_i||J_f|} = \frac{v_i + v_{ky}}{\sqrt{v_{kz}^2 + (v_i + v_{ky})^2}} \tag{5.7}$$

The binary is disrupted if the left hand side of equation 5.3 is non-negative or if the eccentricity as given in equation 5.6 is $e \geq 1$. Succinctly, the binary is disrupted if

$$\frac{v_f}{v_i} \geq \sqrt{\frac{2}{\chi}} \tag{5.8}$$

For any given pre-supernova system, it is necessary to simulate a range of kick velocities and directions to calculate the likelihood of the system becoming unbound. This is a crucial step in this work, as the primary aim is to estimate the percentage of systems that produce a runaway massive star following a supernova explosion.

Chapter 6

Method

A population of binary star systems containing massive stars is synthesised using Monte Carlo techniques with the following prescriptions: the masses of the primaries, in the range $8 - 30\ M_{\odot}$, are distributed according to the power-law IMF of Kroupa (2001); the masses of the secondaries are generated assuming a uniform mass ratio distribution for $q = (M_2/M_1) \in (0, 1]$; the distribution of initial binary separation is flat in $\log a$ with minimum separation $a_{min} = 20\ R_{\odot}$, and maximum separation $a_{max} = 10^5\ R_{\odot}$; an eccentricity of $e = 0$ is assumed in all cases.

The evolution of each binary system from these initial conditions is simulated to determine at which stage of its evolution the primary fills its Roche lobe, followed by implementation of a mass transfer routine based on the stability criteria detailed above and summarised in figure 6.3. It is assumed the primary in the resulting system explodes as a supernova leaving behind a $1.4\ M_{\odot}$ neutron star. Each system is tested for a range of supernova kicks, distributed isotropically with velocities uniformly between $0 - 1000$ kms^{-1}, to determine what percentage of them produce a runaway star with a Betelgeuse-like mass.

Population Synthesis

The sample size for the statistical analysis is 10,000 systems. Masses greater than $30\ M_{\odot}$ are eliminated from the Monte Carlo generator. The effects of the intense stellar superwinds from these stars on the binary companion cannot be neglected, adding a level of complexity beyond the scope of this work. More importantly, these stars will produce black holes, where this work considers only core-collapse supernovae (CCSNe) leaving a remnant neutron star. After elimination, four simulations were performed, totalling 8,361, 8,341, 8,330 and 8,322 binary systems, respectively.

A further simulation was conducted with 1,200 samples, delivering 1,094 valid binary systems, for greater clarity in some of the plots below. Figures 6.1 and 6.2 provide an overview of the initial binary systems under study. Figure 6.1 shows the initial distribution of primary masses from run 4 containing 8,322 samples. Although the number of primaries with $M_1 = 8\ M_{\odot}$ is higher here than other runs (purely a statistical aberration resulting from rounding the generated masses to integer values), the pertinent results from all four simu-

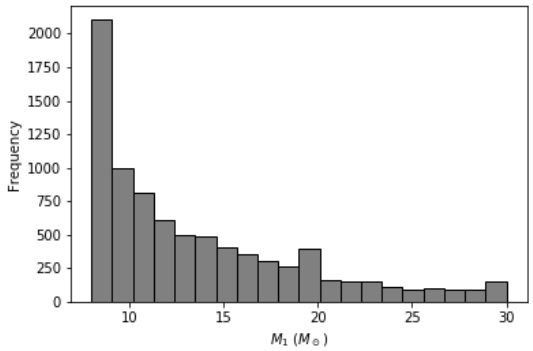

Figure 6.1: The initial distribution of primary masses between 8 $M_\odot$ and 30 $M_\odot$ following the power-law index $\alpha = 2.3$.

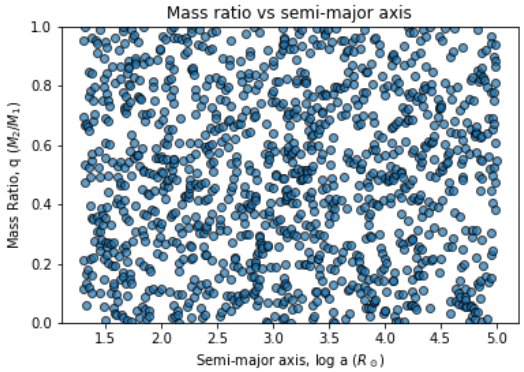

Figure 6.2: The initial distribution of 1,094 binary systems, with mass ratio, $q = M_2/M_1$, versus initial separation in $\log(a)$. In the larger samples the $(q, \log(a))$ space is well-sampled and evenly distributed.

lations differ by less than 2% at each stage of the system evolution. The results reported below represent the mean value from the four runs.

Binary Evolution

Complete HR tracks for single star evolution at integer values between 8 $M_\odot$ and 30 $M_\odot$ were processed from the *Cambridge Stellar Evolution Code* (Church 2020). The main body of code is a self-penned python class *'HR'* (Appendix A) which takes the initial orbital parameters, (M_1, M_2, a) as arguments. From each created instance of a binary system, the code provides methods for establishing if and when RLOF occurs; how mass transfer proceeds; the final pre-SN configuration; and the resulting post supernova outcomes for a range of kick velocities and directions.

Figure 6.3 shows a graphical representation of how each binary is evolved. We first determine if and when the primary fills its Roche lobe. If the Roche lobe is not filled, the component stars evolve as single stars before the more massive star explodes as a supernova. If the Roche lobe is filled on the main sequence, we have case A mass transfer. In our simulation, we are considering massive stars and ignoring the response of the smaller companion. Therefore, we assume case A leads to a contact binary and ultimately a merger. If the Roche lobe is filled after the primary has developed a massive core, we have case B mass transfer. Here we have two branches: if the star is still crossing the Hertzsprung gap, we assume it has a radiative envelope and stable mass transfer ensues if the mass ratio $q \leq 4$. Similarly, if the primary has become a RSG with a convective envelope, we assume stable mass transfer only if mass loss before RLOF has reduced the mass ratio to $q \leq 5/6$. In all other cases, unstable non-conservative mass loss is assumed.

The code determines the updated configuration after mass transfer is complete (which we carry out in one step, neglecting the finer details and complexities). If, on the unstable

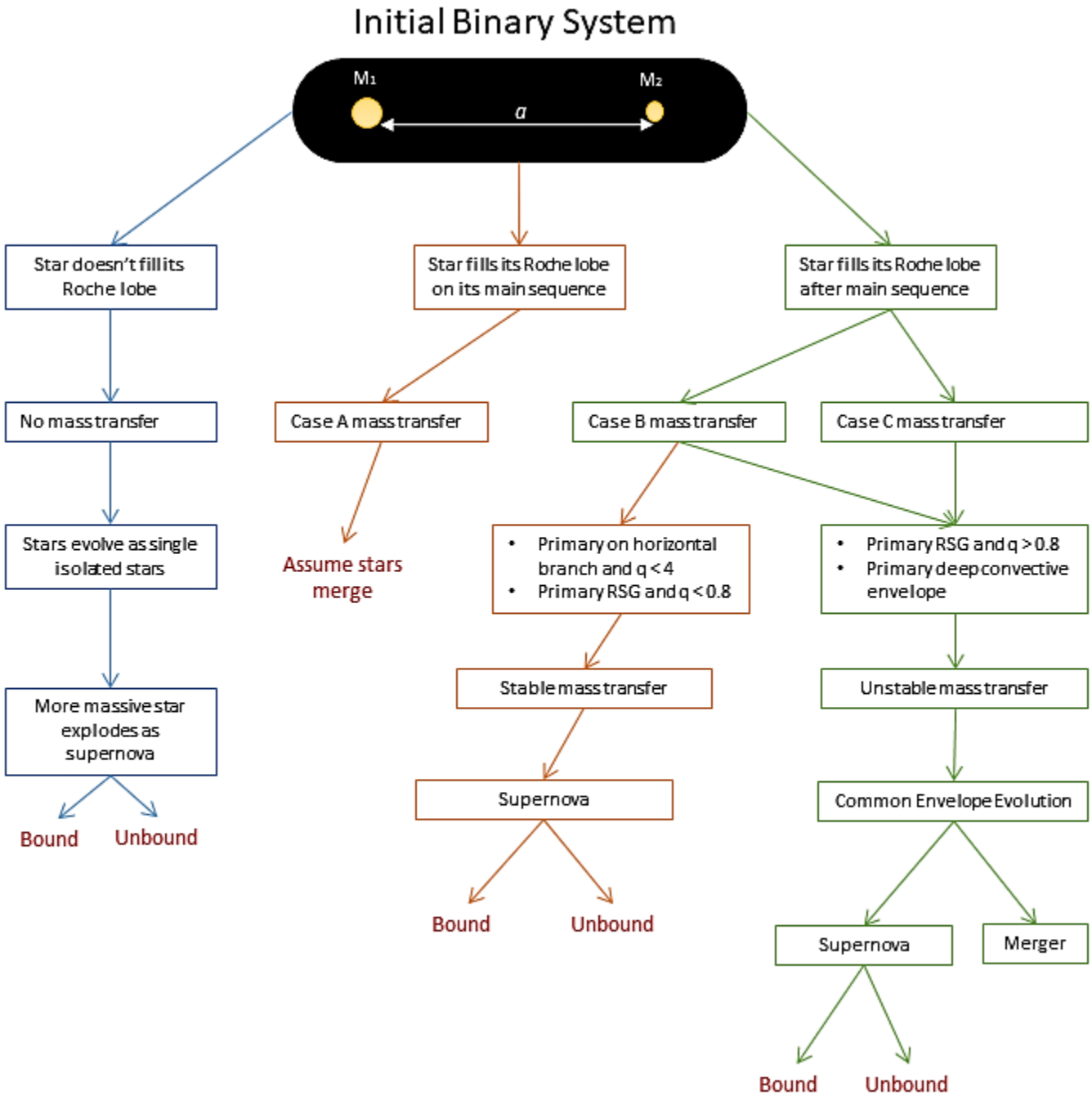

Figure 6.3: The different pathways from initial binary configuration to fully evolved system as explained in the text. The star filling its Roche lobe (or otherwise) is assumed to be the more massive primary.

mass transfer channel, the separation is less than 1 $R_\odot$, we assume a merger. Otherwise, the configurations are taken as the pre-SN orbital elements.

We assume the primary explodes as a supernova shedding all but the 1.4 $M_\odot$ of the remnant neutron star mass. We simulate a range of kicks with velocities from 0 to 1,000 km/s and directions in an isotropic uniform distribution. In total 10^6 kicks are performed for each binary system. The code returns the final total energy, E_{tot} for each kick. The system remains bound if E_{tot} is positive and unbound otherwise. We also determine the minimum kick velocity required to disrupt the system.

Further data analysis and additional functions are performed in Jupyter notebooks with extensive use of pandas dataframes, in particular for plotting and analysing subsets of the data. Again, the key question is what percentage of systems are likely to become unbound, producing a runaway star? Of those systems, how likely is it we have a runaway star in the mass range of Betelgeuse? What can we say about the velocities of those runaway stars? Which evolutionary path best resembles a possible match for Betelgeuse?

Chapter 7

Results & Analysis

7.1 Roche Lobe Overflow

Figure 7.1 shows the relationship between the initial binary configurations (using the smaller sample of 1,094 systems for clarity) and the state of the binary at the onset of RLOF. We find 38.12% of primaries never fill their Roche lobe and the stars evolve as single, non-interacting stars (blue in the figure). As expected, these occur at large initial separations.
For initially very close binaries, RLOF commences during the main sequence of the primary in 3.59% of the systems (red in the figure). The majority of stars (58.29%) fill their Roche lobe having left the main sequence (green in the figure) forming semi-detached binaries.

We see an overlap in close binaries where systems with very similar initial mass ratios and separations reach RLOF at different stages in the evolution of the primary. Figure 7.2 demonstrates how this occurs. We have 3 different binary systems, each with mass ratio $q = 3$ and initial separation $a = 700\ R_\odot$. The initial masses are, however different. Eggleton's formula, equation 4.2, tells us the Roche lobe radius is a function of the mass ratio only for a given separation. Therefore, the three primaries in the figure with masses $8, 12,$ and $18\ M_\odot$ must have approximately the same radius at the onset of RLOF (in this case $\sim 720\ R_\odot$). Clearly the more massive $18\ M_\odot$ will reach this radius at a much earlier stage in its life cycle than the $8\ M_\odot$ star.

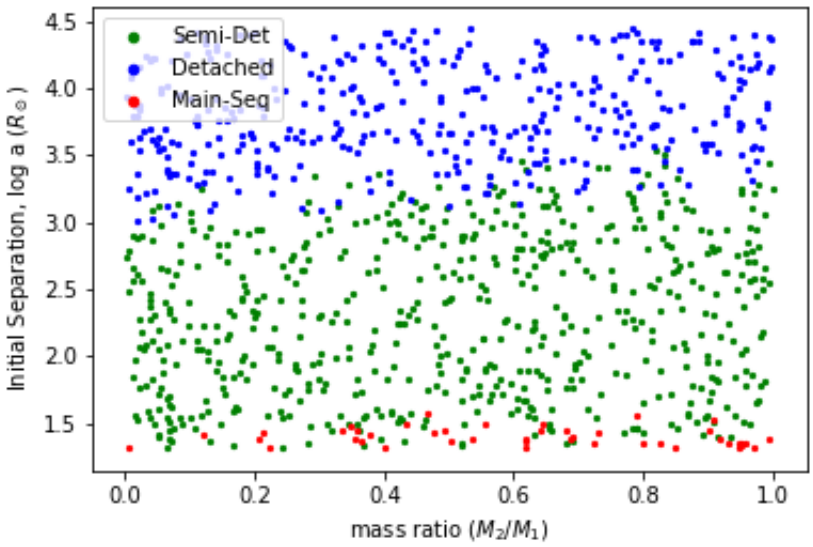

Figure 7.1: Initial separation $\log a$ vs. mass ratio M_2/M_1 for 1,094 binary systems at the onset of RLOF. The primary masses, M_1, are in the range $8 \geq M_\odot \geq 30$. Detached binaries (blue) dominate at larger separations. Short-period binaries with stars that fill their Roche lobe on the main sequence are shown in red. Semi-detached binaries are shown in green.

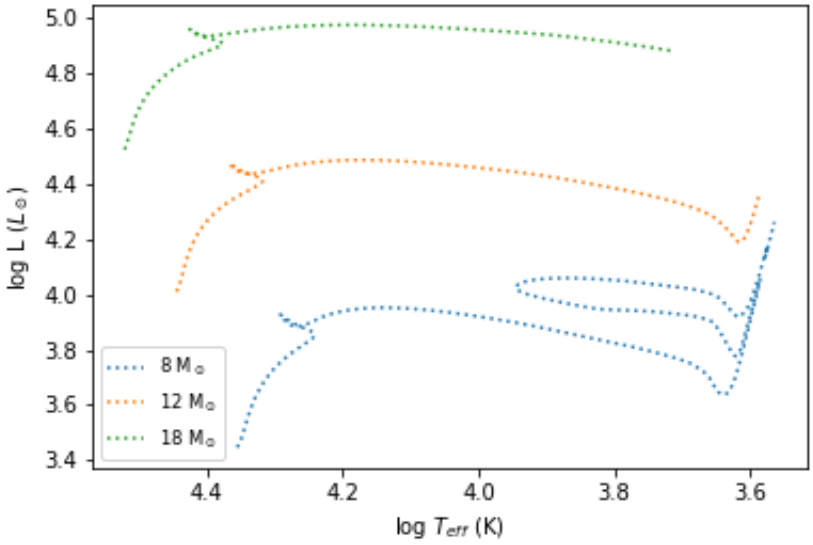

Figure 7.2: HR diagram for 3 primaries with different mass. The mass ratio in each case is $q = M_1/M_2 = 3$ and the initial separation is $a = 700\ R_\odot$. The evolutionary tracks are shown up to the onset of RLOF.

7.2 Mass Transfer

Obviously, in the systems which remain detached, no mass transfer occurs. We also ignore case A mass transfer. This does, in fact, often lead to stable mass transfer. Indeed, in systems where $q \approx 1$, case A mass transfer can be extremely long-lived and stable on the nuclear timescale of the donor. Case A is also thought responsible for Algol systems (Pols 2011). The response of the donor plays a highly significant role in the evolution of such systems. For massive stars, the likelihood of such close companions forming a contact binary is high, and thought to be a major channel in the formation of stellar mergers (Bonnell and Bate 2005), and we assume this outcome here.

For the semi-detached systems, we find 33.42% will lead to stable mass transfer and 24.88% will lead to unstable mass transfer and CEE. Figure 7.3 shows the distribution of the mass transfer types from their initial conditions. Clearly, unstable mass transfer dominates when the primary is much more massive than the secondary. When the mass ratio $q = M_1/M_2$ is smaller, stable mass transfer is dominant at smaller separations. As a increases, we see an increase in unstable mass transfer also at lower mass ratios. This is because RLOF occurs at a later stage in the primary's evolution. Early case B is no longer possible and we see a marked decrease in the proportion of stable mass transfer cases.

In figure 7.4, we see the outcomes of mass transfer. The results are summarised in table 7.1. Of those systems undergoing mass transfer, we find 54.00% undergo stable mass transfer, 25.75% result in a tighter binary after CEE and 20.25% end in a stellar merger. The percentages of the initial population are also in table 7.1.

Table 7.1: Evolutionary path of binary systems. In RLOF, the Semi-Detached column includes all non-case A mass transfer channels. Mass transfer outcomes shows the percentages for the total population (the percentages in brackets are for interacting binaries only, i.e. excluding wide binaries.)

Roche Lobe Overflow		
Main Sequence	Semi-Detached	Detached
3.59%	58.29%	38.12 %
Mass Transfer Type		
Stable	Unstable	No Mass Transfer
33.42%	24.88%	38.12%
Mass Transfer Outcomes		
Stable	Common Envelope	Merger
33.42% (54.00%)	15.94% (25.75%)	12.53% (20.25%)

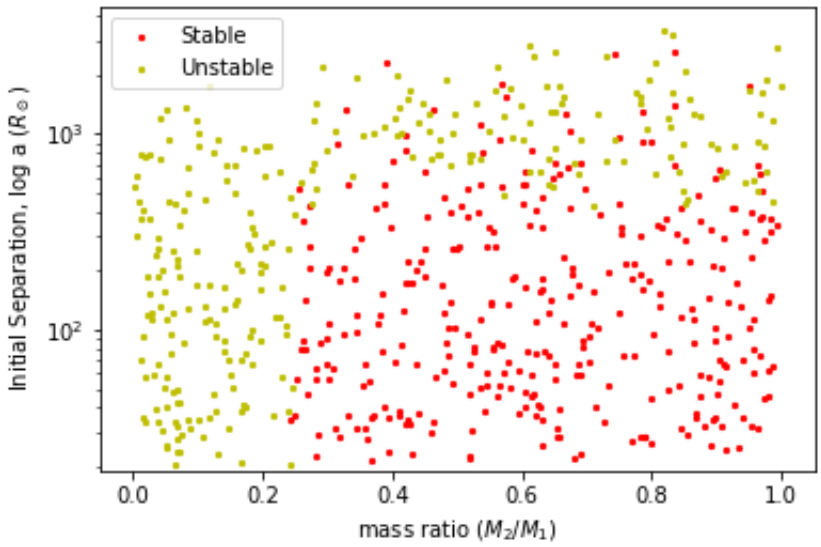

Figure 7.3: Initial separation $\log a$ vs. initial mass ratio (M_2/M_1) for the same sample as in figure 7.1. Stable mass transfer (red) occurs at relatively shorter initial separations and favours secondary masses closer to the primary's. Unstable mass transfer (yellow) arises when the primary is much more massive than the secondary or when the primary has evolved sufficiently to develop a deep convective envelope.

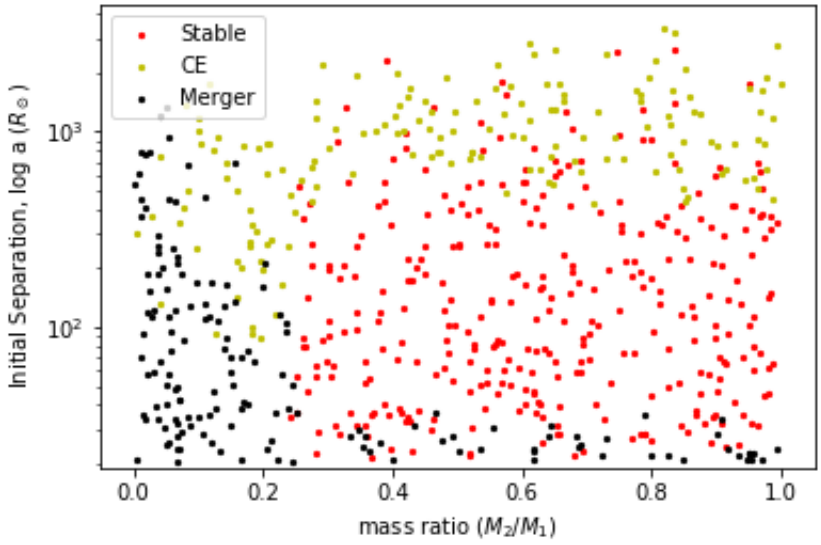

Figure 7.4: Initial separation $\log a$ vs initial mass ratio (M_2/M_1) as in figure 7.3 colour coded for the outcomes of mass transfer. CEE can lead to tighter binaries (yellow) or a merger (black). Stable mass transfer leads to a widening of the orbit (red), or a merger (black) for very close binaries in case A mass transfer.

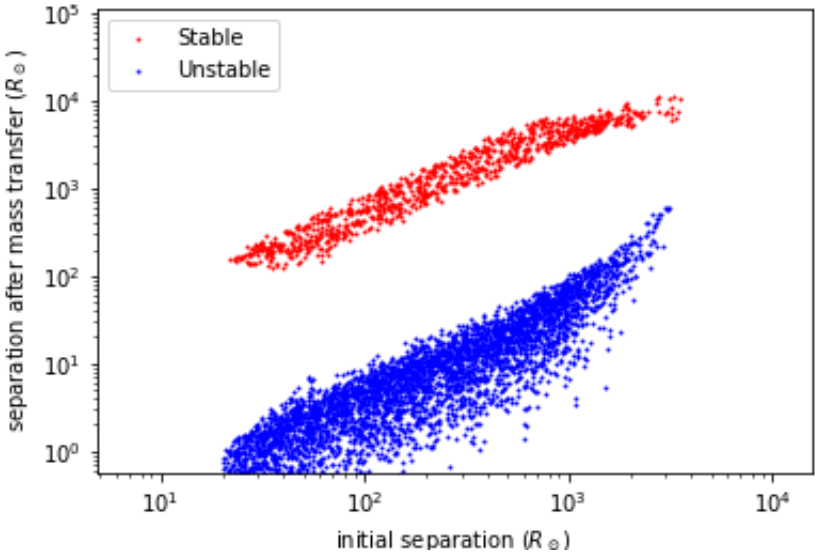

Figure 7.5: The change in separation after mass transfer shows two regimes; widening of the orbit in stable mass transfer (red) and orbital shrinking in unstable mass transfer (green).

Stars which merge after CEE tend to have smaller initial separations and larger mass ratios. From equation 4.12, we see a smaller secondary mass will give a smaller final separation. For larger separations, the primary is also more evolved with a more massive core, which also contributes to the reduction in orbital separation.

In figure 7.5 we see two clearly distinguishable regimes for stable and unstable mass transfer. Stable conservative mass transfer leads to a widening of the orbit (red in the figure). In unstable, non-conservative mass transfer, the orbit always shrinks as discussed above.

7.3 Supernovae

Figure 7.6 illustrates the effect of both the kick velocity and direction in determining whether a particular system remains bound or not. The pre-supernova system has masses $M_1 = 6\ M_\odot$ and $M_2 = 14\ M_\odot$. 10^6 kicks were simulated, distributed isotropically with velocities from 0 to 1,000 km/s. In the extremely tight binary at $a = 1\ R_\odot$, 91.44% of systems remain bound. With an initial separation of $a = 5\ R_\odot$, the percentage of bound systems reduces to 67.96%. At $a = 25\ R_\odot \sim 39\%$ of systems remain bound, while at $a = 100\ R_\odot$, only 18.6% remain bound. The minimum kick velocity (V_{min}) required to disrupt the system always occurs when the kick, $\mathbf{V_k}$ is parallel to the orbital velocity, $\mathbf{V_{orb}}$ and increases with decreasing separation; in this example, V_{min} was calculated to be 473, 214, 95, 49 km/s respectively for $a = 1, 5, 25, 100\ R_\odot$. In the two lower panels of the figure, the separation is large enough, that beyond a certain kick velocity, $\mathbf{V_{max}}$, all systems become unbound, with $\mathbf{V_{max}} = 869$ and 426 km/s for $a = 25$ and 100 $R_\odot$, respectively. In the close binaries of the upper two panels, there is no reasonable kick velocity (i.e. less than 10^3 km/s) that will disrupt every system at arbitrary angles. This is true, in particular, when the kick is antiparallel to the pre-SN orbital velocity. These results assume a uniform distribution of kick velocities; a poor assumption and, in fact, an oversight which I discuss further below.

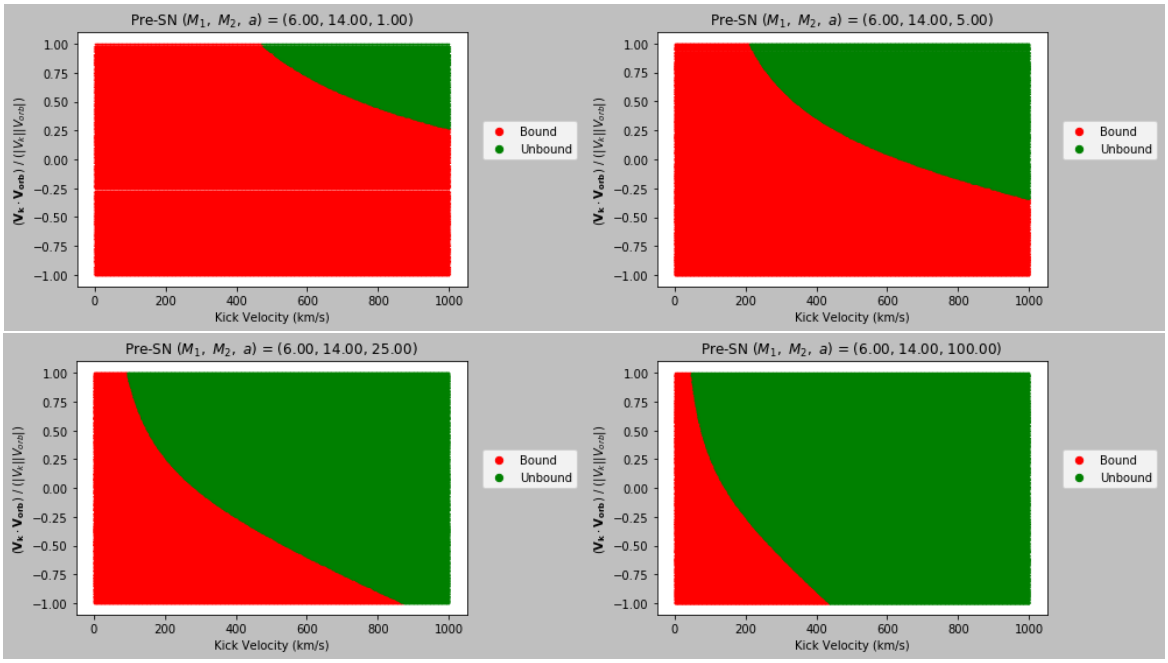

Figure 7.6: For a pre-SN system with $M_1 = 6\ M_\odot, M_2 = 14\ M_\odot$, the percentage of systems which remain bound for a range of supernova kicks depends strongly on the initial separation, a. The y-axis is the normalised dot product of the orbital velocity and supernova kick velocity, effectively $\cos\theta$, where θ is the angle between the two. The x-axis is the magnitude of the kick velocity. *Upper left panel:* The initial separation is 1 $R_\odot$. 91.44% of the systems remain bound; *Upper right panel:* With an initial separation of $a = 5\ R_\odot$, the percentage of bound systems reduces to 67.96%; *Lower left panel:* $a = 25\ R_\odot$ and $\sim 39\%$ of systems remain bound; *Lower right panel:* At $a = 100\ R_\odot$, only 18.6% remain bound.

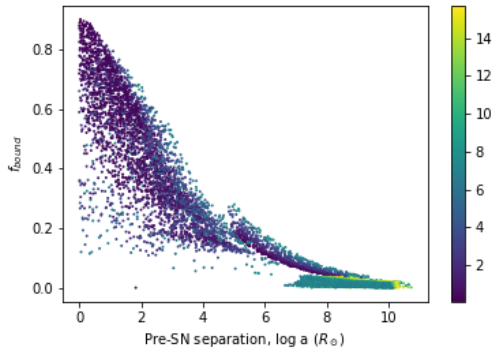

Figure 7.7: The ratio of bound systems versus the pre-supernova separation in all systems undergoing supernova explosions. The colourbar indicates ΔM, the mass lost from the primary during the supernova explosion.

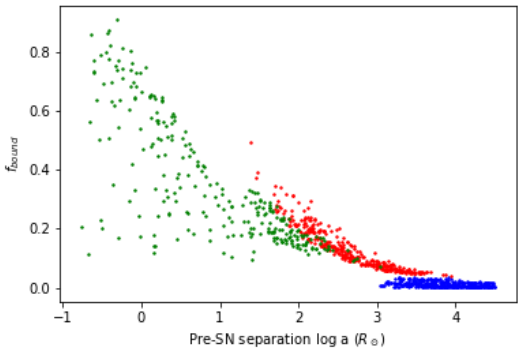

Figure 7.8: The ratio of bound systems versus the pre-supernova separation in systems producing Betelgeuse-like stars, colour-coded by mass transfer type. Wide non-interacting binaries are in blue. Systems evolving from stable mass transfer are shown in red, while those from unstable mass transfer are shown in green.

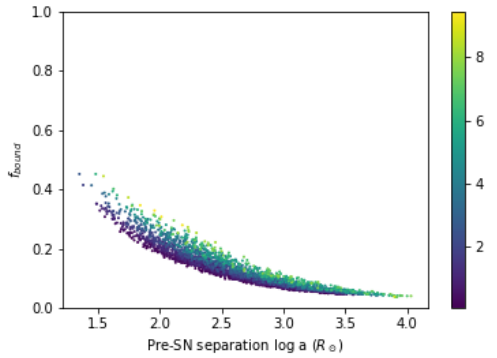

Figure 7.9: The ratio of bound systems versus the pre-supernova separation in systems following stable mass transfer. The colourbar indicates ΔM, the mass lost from the exploding primary.

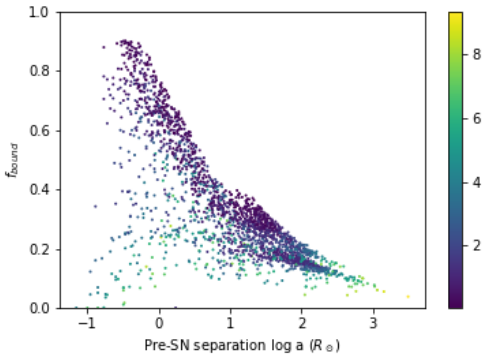

Figure 7.10: The ratio of bound systems versus the pre-supernova separation in systems following unstable mass transfer. The colourbar indicates ΔM, the mass lost from the exploding primary.

Figure 7.7 shows the fraction of bound systems versus separation for all systems in the sample. Figure 7.8 shows the same for systems producing stars with Betelgeuse-like masses, colour-coded by mass transfer type. The three regimes of unstable, stable and no mass transfer are clearly defined and in agreement with the expectation that tighter binaries following CEE are more difficult to disrupt, whereas wide binaries are only weakly bound. Table 7.2 shows the mean value for disrupted systems for each of the mass transfer channels.

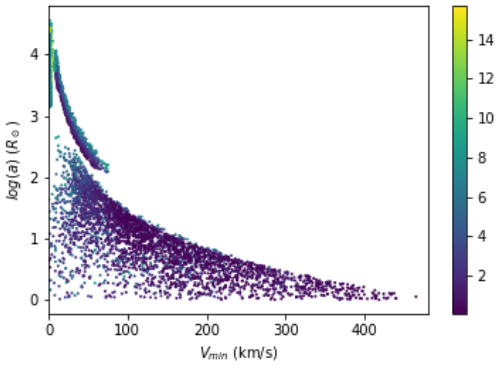

Figure 7.11: The minimum kick velocity required to disrupt a binary system versus the pre-SN separation. The colour-bar indicates the value for ΔM.

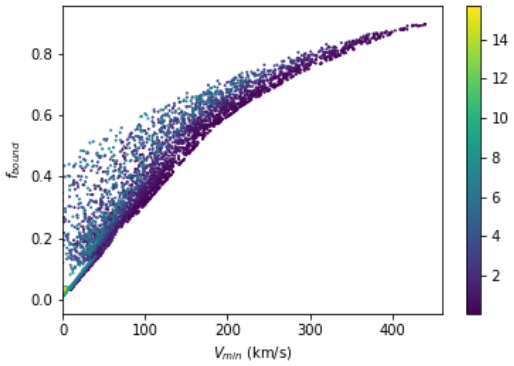

Figure 7.12: The ratio of bound systems versus the minimum kick velocity required to disrupt the system. The colour-bar indicates the value for ΔM.

Figures 7.9 and 7.10 show the fraction of bound systems as a function of the separation for the stable and unstable mass transfer channels, respectively. The unstable channel shows a clear correlation between the mass lost in the supernova ΔM and the number of unbound systems at a given separation. For stable mass transfer, the relationship for ΔM appears reversed. Systems undergoing stable mass transfer will have wider orbits. For increasing pre-SN separation, the secondary's mass is, on average, proportionally higher (as can be seen in table 7.5) as it has accreted more mass. In addition, the core mass of the primary before the supernova is invariably small. This is quite apparent if one compares the values in tables 7.5 and 7.4 which are randomised samples from the Betelgeuse-like populations for stable and unstable mass transfer, respectively. Typically then, the pre-SN potential energy will be dominated by the comparative mass of the secondary. What remains true is that, for a given ΔM, the number of bound systems falls off with the orbital separation.

Figure 7.11 shows the relation between the minimum kick required to disrupt the system and the orbital separation. Smaller separations require larger kicks. The colour bar in the figure represents the mass lost from the exploding star, ΔM. For higher values of ΔM, no kick is required if the condition $\Delta M > (1/2)(M_1 + M_2)$ is satisfied. In figure 7.12 the proportion of bound systems is plotted as a function of the minimum kick required to disrupt

Table 7.2: Global sample of post-supernova systems by mass transfer type, including wide (non-interacting) binaries. The mean and median of unbound systems are given in percentages for a range of 10^6 kicks up to 1000 km/s for each system over the entire sample.

Mass Transfer	Mean Unbound (%)	Median Unbound (%)
Stable	86.80	88.50
Unstable	66.04	72.70
Wide	98.72	98.90

the system. For tightly bound systems, larger minimum kicks are necessary. Again, for large ΔM, systems are unbound more readily.

In the next section, we move from these global statistics to systems producing Betelgeuse-like stars.

7.4 Final Outcomes

In total we find that 14.03% of the initial binary systems will produce a secondary with a stellar mass in the range $13 \leq M/M_{\odot} \leq 18$, excluding mergers. 12.77% of the total initial population produce a runaway star of appropriate mass. Of those systems with Betelgeuse-like candidates, 74.92% arise from the stable mass transfer channel, 6.18% from unstable mass transfer and 18.90% emerge from detached binary systems.

Noting the uncertainty in Betelgeuse's current mass and increasing the range of stellar masses to $11 \leq M/M_{\odot} \leq 20$ produces a significant increase to 25.18% of systems with possible candidates and 22.87% with runaway stars. Of these, 77.92% are found in the stable mass transfer channel, 5.71% in the unstable mass transfer channel and 16.39% are from non-interacting binary systems. Figures 7.13 and 7.14, focus on the stable and unstable mass transfer channels, respectively.

Table 7.3 shows the mean and median values of the percentage of unbound systems in each of the mass transfer channels. We find that wide binaries will nearly always disrupt after a supernova explosion with on average $> 97\%$ producing a runaway star. Systems following the stable mass transfer channel tend to also have comparatively wide pre-SN orbital separations and we find $\sim 90\%$ will be disrupted. Unstable mass transfer leads to tighter binary systems which are more difficult to disrupt in the supernova. For the chosen range of kicks, we find 84.89% of systems are disrupted. This seems a high number, but reducing the range of kick velocities to a maximum of 500 km/s, we find a mean value of 34.76% of unbound systems. Clearly the equal weighting of natal kick velocities across the $0-1000$ km/s range emphasises the import of the kick velocity in disrupting the system. Indeed, the uniform distribution of kick velocities was an oversight on my part. The distribution of kick velocities has been found to be well described by a Maxwellian distribution (Hobbs et al. 2005) with mean velocities between $200-500$ km/s (Limongi 2017; Villaume et al. 2017). Our results are certainly then a substantial overestimation of the number of unbound systems produced in a typical system.

Nevertheless, the results strongly suggest stable mass transfer as the most likely source of large mass runaway stars. This is in part due to the not insignificant number of ZAMS intermediate mass stars in such systems which accrete mass from a more massive partner. These stars will experience rejuvenation and, in effect, become massive main sequence stars.

In our simple model where companions in unstable mass transfer do not accrete matter, there is then no addition to the intial population of massive secondaries in these systems. Coupled with the possibility of mergers and tightly bound systems, we expect to see propor-

tionally fewer runaway stars from these systems.

Figures 7.15 and 7.16 trace the Betelgeuse candidates to their initial conditions from the stable and unstable channels, respectively. In the unstable channel, originally close binary systems tend to have large mass ratios and will ultimately merge. Even those secondaries that survive the CE phase will have comparatively small mass. Our Betelgeuse candidates from this channel then invariably stem from relatively wide binaries, preferentially with lower mass ratios. In the stable channel, high mass ratios are absent since mass transfer in such systems will generally be unstable. The most general conclusion to be drawn from the stable channel is that the Betelgeuse candidates are found more often at initial separations less than 300 $R_\odot$ and mass ratios M_2/M_1 between 0.8 and 1.

The rightmost column in tables 7.4 and 7.5 gives the pre-SN velocity of the secondary star in systems following unstable and stable mass transfer, respectively. In the former, the velocities are on average much higher. As discussed, CEE will form tighter binaries with initially more massive primaries, and consequently more massive cores than those systems evolving on the stable mass transfer channel. The post-SN binary will be unbound only if the kinetic energy exceeds the potential energy. The smaller the separation, the larger the kick required to disrupt the system. Detailed calculations performed by Tauris and Takens (1998) have established that runaway velocities of companion stars are correlated with the magnitude and direction of the kick away from the companion. Only in close binaries does the shell velocity impact on the companion's runaway velocity.

The mean orbital velocity of Betelgeuse candidates in the unstable channel is found to be $\langle V_2 \rangle = 34.71$ km/s. The mean minimum kick velocity is $\langle V_{min} \rangle = 37.67$ km/s. Most of these systems require a reasonable kick velocity to become unbound, and have secondaries with speeds greater than the observed ~ 30 km/s of Betelgeuse.

The mean velocity of candidates in the stable channel is $\langle V_2 \rangle = 15.55$ km/s. The mean minimum kick velocity is $\langle V_{min} \rangle = 37.30$ km/s. The smaller average values of the orbital speeds of the secondaries necessitates larger kick velocities to match the observed speed of Betelgeuse, particularly for those with larger separations.

Table 7.3: The mean and median percentage of unbound systems where the secondary is a Betelgeuse-like star for each mass transfer channel.

Mass Transfer	Mean Unbound (%)	Median Unbound (%)
Stable	89.80	90.90
Unstable	84.89	83.10
Wide	97.68	97.75

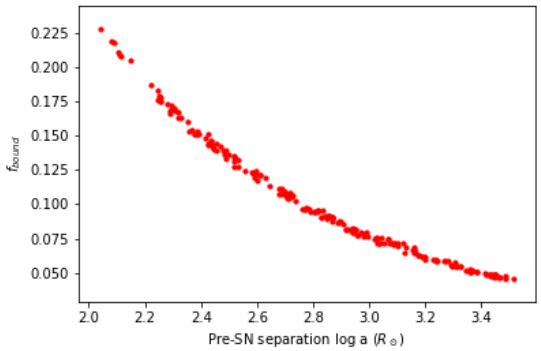

Figure 7.13: The ratio of bound systems versus the pre-supernova separation in systems containing Betelgeuse-like secondaries, following the stable mass transfer channel.

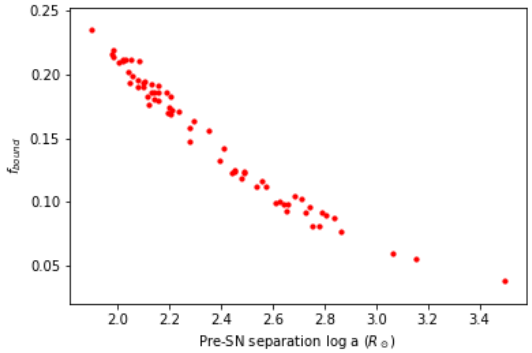

Figure 7.14: The ratio of bound systems versus the pre-supernova separation in systems containing Betelgeuse-like secondaries, following the unstable mass transfer channel.

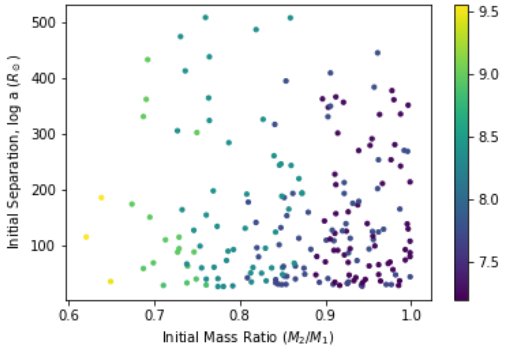

Figure 7.15: The initial binary configuration for systems containing Betelgeuse-like stars post-supernova. The colourbar indicates the change in mass following accretion during stable mass transfer.

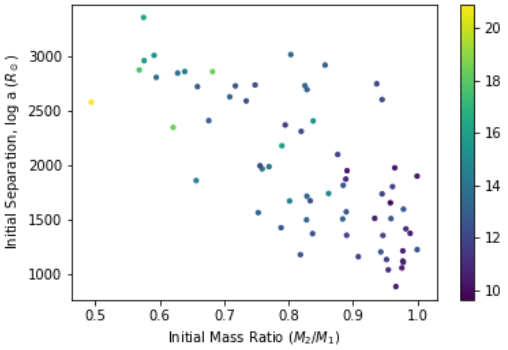

Figure 7.16: The initial binary configurations for systems evolving common envelopes before producing Betelgeuse-like stars post-supernova. The colourbar indicates the mass lost from the primary during mass transfer, i.e. the primary's envelope mass.

7.4.1 Example

We consider two channels producing a runaway star of mass $M_2 \approx 16\ M_\odot$. System 1 has initial masses $M_1 = 10\ M_\odot$ and $M_2 = 9\ M_\odot$ and initial orbital period of 170 days, i.e. the initial separation is 100 $R_\odot$. The primary fills its Roche lobe as it crosses the Hertzsprung gap (figure 7.17). It has developed a massive core but maintains its radiative envelope. Mass transfer ensues according to early case B mass transfer. Since the mass ratio $q = 1.11 \leq 4$, we have conservative, stable mass transfer. Assuming the mass transfer continues until the primary is stripped of its envelope, all of which is accreted by the companion, upon completion of mass transfer, the primary has a core mass of $M_{1,core} = 2.03\ M_\odot$, while the secondary has become a significantly more massive mains sequence star with $M_2 = 16.76\ M_\odot$. The binary experiences significant widening during mass transfer and the separation is now $a = 675.69\ R_\odot$. We assume this configuration as the pre-supernova configuration. The primary explodes as a supernova leaving behind a neutron star of mass $M_{NS} = 1.4\ M_\odot$. The mass lost to the system is $\Delta M = M_{1,core} - M_{NS} = 0.63\ M_\odot$. For an isotropic distribution of kick directions, ranging in velocity from 0 to 1000 km/s, we find 7.46% of the systems remain bound and 92.54% become unbound. The minimum kick required to disrupt the system is 29.0 km/s (parallel to the orbital motion) and the maximum kick, beyond which all systems are unbound, is found to be 273.0 km/s. The most likely outcome of such a system is thus a neutron star of mass $M_{NS} = 1.4\ M_\odot$ and a runaway massive star $M_2 \sim 16 - 17\ M_\odot$

System 2 has initial masses $M_1 = 22\ M_\odot$ and $M_2 = 16\ M_\odot$. The initial separation is $a = 2500\ R_\odot$. In this case the primary fills its Roche lobe at a much more evolved state, on the red supergiant branch (figure 7.18). Helium core ignition has commenced and the primary has developed a deep convective core. Mass transfer ensues as case C, dynamically unstable mass transfer. The system develops a common envelope. If we assume the secondary does not accrete matter during formation of the envelope, the pre-supernova masses are then, $M_{1,core} = 6.24\ M_\odot$ and $M_2 = 16\ M_\odot$. Friction and angular momentum loss causes the stars to spiral in, resulting in a tighter binary with final separation of $a = 218.20\ R_\odot$. Again the primary explodes as a supernova leaving behind a neutron star. The mass lost to the system in this case is $\Delta M = 4.84\ M_\odot$. Approximately 14.26% of the systems will remain bound, with 85.74% unbound. The minimum kick required to unbind the system is 36.0 km/s and no systems remain bound with kicks exceeding 312.0 km/s.

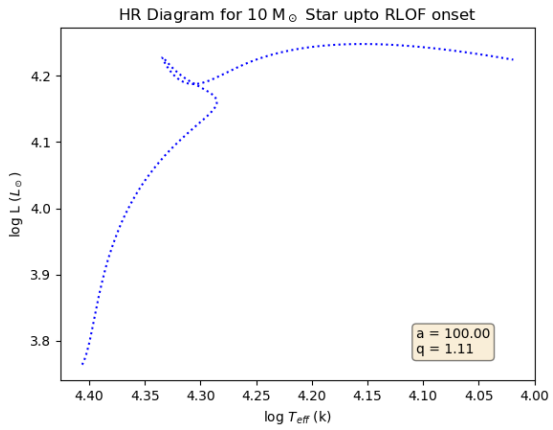

Figure 7.17: HR diagram for a 10 $M_\odot$ primary and 9 $M_\odot$ secondary with initial separation 100 $R_\odot$. The primary fills its Roche lobe crossing the Hertzsprung gap.

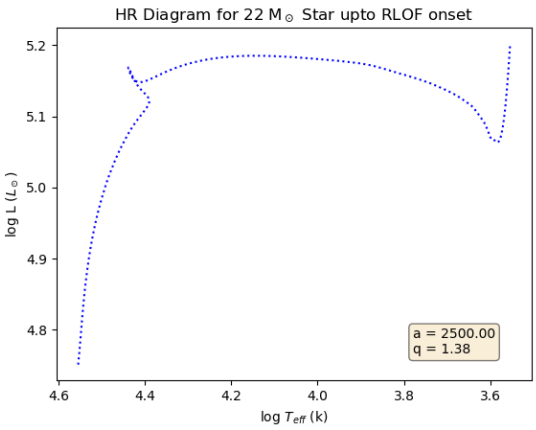

Figure 7.18: HR diagram for a 22 $M_\odot$ primary and 16 $M_\odot$ secondary, with initial separation 2500 $R_\odot$. The primary fills its Roche lobe on the Red Supergiant Branch.

Table 7.4: Representative sample of systems with secondaries of mass $11 < M_2 < 20$ following the non-conservative mass transfer channel. Masses are given in units of $M_\odot$ and distance in units of $R_\odot$. The left panel and centre panel give the initial and pre-SN orbital elements respectively. The right panel contains the proportion of unbound systems for a range of kicks as described in the text, the minimum kick velocity required to disrupt the system and the pre-SN orbital velocity of the secondary in km/s.

$M_{1,i}$	$M_{2,i}$	a_i	$M_{1,SN}$	$M_{2,SN}$	a_{SN}	$Unbound$	V_{min}	V_2
12	11.42	1672.34	3.61	11.42	228.54	0.87	34.22	26.85
23	18.86	3380.82	8.67	18.86	1096.66	0.93	14.73	21.75
18	17.61	1915.01	4.71	17.61	188.76	0.83	45.74	31.63
23	14.24	2513.00	6.50	14.24	187.83	0.85	33.04	45.39
13	12.99	1772.46	4.00	12.99	266.04	0.87	33.22	25.93
19	11.07	1712.78	5.07	11.07	105.93	0.82	41.36	53.45
16	12.41	1619.95	4.14	12.41	125.19	0.82	46.25	39.65
21	15.36	2517.11	7.60	15.36	519.87	0.90	19.08	30.32
21	13.69	2597.73	7.61	13.69	487.74	0.91	17.34	32.54
13	12.63	1626.12	4.00	12.63	236.84	0.87	34.54	27.78
13	12.66	877.77	3.07	12.66	74.81	0.76	67.36	39.01
27	16.54	2858.29	7.94	16.54	236.46	0.86	29.54	45.49
18	17.87	2794.07	6.00	17.87	548.83	0.90	24.61	22.85
12	11.61	1255.36	2.69	11.61	100.44	0.80	57.39	30.94
22	18.74	2096.57	6.10	18.74	203.48	0.83	41.64	37.40
21	16.74	1905.33	5.75	16.74	168.09	0.82	43.07	40.76
22	17.75	2315.51	6.10	17.75	213.53	0.84	38.93	37.26
18	11.82	1758.96	4.71	11.82	118.09	0.82	43.17	46.47
22	12.38	2175.90	6.11	12.38	141.72	0.84	34.77	52.03
14	11.67	1630.90	4.37	11.67	214.61	0.87	32.96	32.47

Table 7.5: Representative sample of systems with secondaries of mass $11 < M_2 < 20$ following the conservative mass transfer channel. Masses are given in units of $M_\odot$ and distance in units of $R_\odot$. The left panel and middle panel give the initial and pre-SN orbital elements of the binary, respectively. The right panel gives the proportion of unbound systems for a range of kicks as described in the text, the minimum kick velocity required to disrupt the system and the pre-SN velocity (V_2) of the secondary in the COM-frame in km/s.

$M_{1,i}$	$M_{2,i}$	a_i	$M_{1,SN}$	$M_{2,SN}$	a_{SN}	$Unbound$	V_{min}	V_2
9	3.84	33.02	1.78	11.06	101.90	0.80	60.83	21.45
8	5.56	81.56	1.46	12.10	516.54	0.91	29.04	7.60
8	5.46	58.49	1.47	11.99	360.98	0.89	34.55	9.19
11	4.35	23.67	2.51	12.61	52.72	0.72	84.35	38.75
11	2.94	140.66	2.36	11.33	201.37	0.86	41.34	19.59
8	6.83	28.95	1.49	13.34	218.00	0.85	46.60	11.42
11	8.89	342.94	2.34	17.28	1927.74	0.94	16.71	5.24
8	7.13	25.68	1.50	13.63	199.69	0.85	49.14	11.89
10	3.25	95.83	2.03	11.02	197.43	0.86	42.54	17.43
12	6.83	540.87	2.70	15.83	1923.33	0.94	15.57	6.23
12	10.46	490.85	2.70	19.45	2696.51	0.95	14.70	4.82
10	9.27	416.48	2.02	17.05	2940.84	0.95	13.73	3.72
9	3.98	226.07	1.74	11.25	762.69	0.92	22.50	7.62
13	10.18	28.52	3.26	19.69	118.17	0.77	68.33	27.29
10	3.44	96.50	2.03	11.20	214.76	0.86	41.12	16.60
10	6.57	28.16	2.09	14.28	133.16	0.81	58.70	19.51
10	7.84	190.54	2.02	15.61	1139.77	0.93	21.10	6.21
9	8.85	150.13	1.74	16.11	1209.83	0.93	21.21	5.16
8	5.22	55.34	1.47	11.75	324.60	0.89	36.10	9.78
12	6.08	424.32	2.70	15.08	1317.67	0.94	18.31	7.69

Chapter 8

Conclusion

Every paper on astrophysics comes with caveats. We are unable to observe systems evolving over time, but must rely on simulations and comparative studies, testing outcomes with observations. The results necessarily depend on the underlying assumptions made in each model. Chiefly, then, the goal is often to further constrain the uncertainties in some hoped-for standard model. This is particularly true for massive stars, given their short lifespans and relative paucity. The myriad of interactions in binary systems, where most massive stars reside, and dense clusters only serves to complicate the picture further.

In this work, we have made some extreme simplifications. We assume all stable mass transfer is conservative, thereby neglecting the responses of donor and companion stars during mass transfer, where the mass ratio may be reversed, the companion may fill its Roche lobe, or some mass or angular momentum may be lost from the system.

In unstable mass transfer, we assume the companion star does not accrete mass and that energy is not lost from the system - an unlikely scenario.

Wide binaries are very likely to produce runaway stars. However, if we assume a secondary mass of about 16 $M_{\odot}$ evolving as a single star, its companion must be a more massive, short-lived star. To place such a system's birthplace in Orion OB1a and allow sufficient time to observe a Betelgeuse-like star so far from 'home' necessitates some fine-tuning, unless the binary system itself was ejected soon after formation. This may occur for some systems, but one could speculate that few wide binaries would remain intact after dynamical ejection (of course, we would still have a runaway star, but the fingerprints of binary interactions, such as rapid rotation, would be absent).

Are our results, then, little more than back-of-an-envelope estimates? To first approximation, they contain the most important underlying physical processes. At every juncture in the evolution of our model, we can add complexity which will alter subsequent evolution in various ways. As mentioned, we could/should weigh our supernova kick velocities to reflect the observed/inferred mean kick velocities and Maxwellian distribution, which would significantly reduce the proportion of systems producing massive runaway stars.

Sana et al. (2012) found that approximately 30% of massive stars in binaries will end in a merger, significantly higher than our result of $\sim 13\%$. Again, the simplified energy formalism of CEE produces different results than a more complex γ formalism, incorporating non-conservative mass transfer modes, for example. Additionally, we adopted an extremely conservative stellar radius of $\leq 1\ R_\odot$ as a condition for a merger. Even for a star stripped entirely of its envelope, the radius of the remaining core is likely to be significantly larger for the more massive stars in our sample.

Betelgeuse as a Merger? In this paper, we have looked exclusively at the case of Betelgeuse as the smaller companion in a massive binary system. Chatzopoulos et al. (2020) have examined the possibility that Betelgeuse was in fact a $15 - 17\ M_\odot$ primary which merged with a smaller $1 - 4\ M_\odot$ companion. They propose the binary system was ejected intact from its birthplace a few million years ago before a merger took place some hundreds of thousands of years ago when Betelgeuse was crossing the Hertzsprung gap. The primary goal of their paper is to explain Betelgeuse's unexpectedly fast rotation rate, which we have here neglected. They explicitly do not rule out spin up by accretion (with Betelgeuse as the smaller companion) and subsequent ejection in a supernova explosion.

Of course, there are other channels for producing runaway stars. A solitary star may stray too close to a massive binary and be slung-shot from its parent cluster. Alternatively, a companion star in a binary may have already experienced interactions with its partner, before a subsequent interaction with another binary or a wandering massive star may kick the star from its system.

Fujii and Portegies Zwart (2011) report $\sim 20\%$ of massive OB stars are observed with significant peculiar velocities with Gvaramadze and Gualandris (2011) reporting up to 25% of runaways among spectral-type O stars. Whether the main mechanism for such ejections from the parent cluster is by dynamical slingshot or through binary disruption during a supernova event is not easily discernible, since the observed runaway stars are often far from their birth place. Both of the aforementioned papers suggest a significant proportion of massive stars are dynamically ejected early in the evolution of young star clusters and this mechanism is chiefly responsible for runaways with higher velocities (above 30 km/s). Further production of massive runaways in supernova explosions occurs later and Fujii and Portegies Zwart (2011) model hardening of massive binaries within the cluster which may, themselves, be subsequently ejected from the birth environment. Either way, they propose the relative fraction of runaway stars is inversely proportional to the total mass of the cluster. A truer representation of the processes producing a massive runaway like Betelgeuse clearly requires incorporation of a broader field of investigation than simple binary interactions for an effective comparative study.

Adding such complexity is beyond the scope of this work. Our conclusion that the most likely channel for producing a massive runaway star in binaries is by stable mass transfer is at least plausible. It broadens the scope for ZAMS intermediate mass stars to subsequently evolve as massive main sequence stars before its companion explodes as a supernova. It is

also less likely to produce mergers and, perhaps most importantly, it produces wider, more loosely bound pre-SN systems with stars of the appropriate mass. That this occurs in up to 25% of systems places such stars in the category of rare, but certainly not unusual. It is safe to assume that, although we cannot say for certain how Betelgeuse itself has evolved, the production of massive runaway stars in binary systems is not an atypical phenomenon.

Bibliography

Bonnell, Ian A. and Matthew R. Bate (Sept. 2005). "Binary systems and stellar mergers in massive star formation". In: *MNRAS* 362.3, pp. 915–920. DOI: 10.1111/j.1365-2966.2005.09360.x. arXiv: astro-ph/0506689 [astro-ph].

Brandt, W. N. and Ph. Podsiadlowski (Dec. 1994). "The Effects of High-Velocity Supernova Kicks on the Orbital Properties and Sky Distributions of Neutron Star Binaries". In: *arXiv e-prints*, astro-ph/9412023, astro–ph/9412023. arXiv: astro-ph/9412023 [astro-ph].

Chatzopoulos, E. et al. (May 2020). "Is Betelgeuse the Outcome of a Past Merger?" In: *arXiv e-prints*, arXiv:2005.04172, arXiv:2005.04172. arXiv: 2005.04172 [astro-ph.SR].

Chiosi, Cesare and Andre Maeder (Jan. 1986). "The evolution of massive stars with mass loss." In: *ARA&A* 24, pp. 329–375. DOI: 10.1146/annurev.aa.24.090186.001553.

Church, Ross (2020). *HR Tracks from Cambridge Stellar Evolution Code (personal communication)*.

Eggleton, P. P. (May 1983). "Aproximations to the radii of Roche lobes." In: *ApJ* 268, pp. 368–369. DOI: 10.1086/160960.

Eldridge, J. J. (2017). "Population Synthesis of Massive Close Binary Evolution". In: *Handbook of Supernovae*. Ed. by Athem W. Alsabti and Paul Murdin. Cham: Springer International Publishing, pp. 671–692. ISBN: 978-3-319-21846-5. DOI: 10.1007/978-3-319-21846-5_125. URL: https://doi.org/10.1007/978-3-319-21846-5_125.

Fujii, Michiko S. and Simon Portegies Zwart (Dec. 2011). "The Origin of OB Runaway Stars". In: *Science* 334.6061, p. 1380. DOI: 10.1126/science.1211927. arXiv: 1111.3644 [astro-ph.GA].

Geha, Marla et al. (July 2013). "The Stellar Initial Mass Function of Ultra-faint Dwarf Galaxies: Evidence for IMF Variations with Galactic Environment". In: *ApJ* 771.1, 29, p. 29. DOI: 10.1088/0004-637X/771/1/29. arXiv: 1304.7769 [astro-ph.CO].

Gvaramadze, Vasilii V. and Alessia Gualandris (Jan. 2011). "Very massive runaway stars from three-body encounters". In: *MNRAS* 410.1, pp. 304–312. DOI: 10.1111/j.1365-2966.2010.17446.x. arXiv: 1007.5057 [astro-ph.SR].

Harper, G. M. et al. (July 2017). "An Updated 2017 Astrometric Solution for Betelgeuse". In: *AJ* 154.1, 11, p. 11. DOI: 10.3847/1538-3881/aa6ff9. arXiv: 1706.06020 [astro-ph.SR].

Heuvel, Edward P. J. van den (2017). "Supernovae and the Evolution of Close Binary Systems". In: *Handbook of Supernovae*. Ed. by Athem W. Alsabti and Paul Murdin. Cham: Springer International Publishing, pp. 1527–1554. ISBN: 978-3-319-21846-5. DOI: 10.1007/978-3-319-21846-5_75. URL: https://doi.org/10.1007/978-3-319-21846-5_75.

Hobbs, G. et al. (July 2005). "A statistical study of 233 pulsar proper motions". In: *MNRAS* 360.3, pp. 974–992. DOI: 10.1111/j.1365-2966.2005.09087.x. arXiv: astro-ph/0504584 [astro-ph].

Hurley, Jarrod R., Christopher A. Tout, and Pols. (Feb. 2002). "Evolution of binary stars and the effect of tides on binary populations". In: *MNRAS* 329.4, pp. 897–928. DOI: 10.1046/j.1365-8711.2002.05038.x. arXiv: astro-ph/0201220 [astro-ph].

Hut, P. (Dec. 1980). "Stability of tidal equilibrium". In: *A&A* 92.1-2, pp. 167–170.

Karttunen, Hannu et al. (2017). *Fundamental Astronomy*. DOI: 10.1007/978-3-662-53045-0.

Kroupa, Pavel (Apr. 2001). "On the variation of the initial mass function". In: *MNRAS* 322.2, pp. 231–246. DOI: 10.1046/j.1365-8711.2001.04022.x. arXiv: astro-ph/0009005 [astro-ph].

Kroupa, Pavel and Andreas Burkert (July 2001). "On the Origin of the Distribution of Binary Star Periods". In: *ApJ* 555.2, pp. 945–949. DOI: 10.1086/321515. arXiv: astro-ph/0103429 [astro-ph].

Kroupa, Pavel, Carsten Weidner, et al. (2013). "The Stellar and Sub-Stellar Initial Mass Function of Simple and Composite Populations". In: *Planets, Stars and Stellar Systems. Volume 5: Galactic Structure and Stellar Populations*. Ed. by Terry D. Oswalt and Gerard Gilmore. Vol. 5, p. 115. DOI: 10.1007/978-94-007-5612-0_4.

Kulkarni, S.R. (2010). *Supernovae in Binary Systems: Orbital Dynamics*.

Leahy, Denis A. and Janet C. Leahy (May 2015). "A calculator for Roche lobe properties". In: *Computational Astrophysics and Cosmology* 2, 4, p. 4. DOI: 10.1186/s40668-015-0008-8.

Levesque, Emily M (2017). *Astrophysics of Red Supergiants*. 2514-3433. IOP Publishing. ISBN: 978-0-7503-1329-2. DOI: 10.1088/978-0-7503-1329-2. URL: http://dx.doi.org/10.1088/978-0-7503-1329-2.

Limongi, Marco (2017). "Supernovae from Massive Stars". In: *Handbook of Supernovae*. Ed. by Athem W. Alsabti and Paul Murdin. Cham: Springer International Publishing, pp. 513–565. ISBN: 978-3-319-21846-5. DOI: 10.1007/978-3-319-21846-5_119. URL: https://doi.org/10.1007/978-3-319-21846-5_119.

McKee and Tan (Mar. 2002). "Massive star formation in 100,000 years from turbulent and pressurized molecular clouds". In: *Nature* 416.6876, pp. 59–61. DOI: 10.1038/416059a. arXiv: astro-ph/0203071 [astro-ph].

Meynet, G. et al. (May 2013). "The past and future evolution of a star like Betelgeuse". In: *EAS Publications Series*. Ed. by P. Kervella, T. Le Bertre, and G. Perrin. Vol. 60. EAS Publications Series, pp. 17–28. DOI: 10.1051/eas/1360002. arXiv: 1303.1339 [astro-ph.SR].

Moeckel, Nickolas and Cathie J. Clarke (Feb. 2011). "Collisional formation of very massive stars in dense clusters". In: {}*mnras* 410.4, pp. 2799–2806. DOI: 10.1111/j.1365-2966.2010.17659.x. arXiv: 1009.0283 [astro-ph.SR].

Nelson, C. A. and P. P. Eggleton (May 2001). "A Complete Survey of Case A Binary Evolution with Comparison to Observed Algol-type Systems". In: *ApJ* 552.2, pp. 664–678. DOI: 10.1086/320560. arXiv: astro-ph/0009258 [astro-ph].

Neustroev, Vitaly (2017). *Astrophysics of Interacting Binary Stars (Lecture Notes)*.

Parker, Richard J. (2017). "The Effects of Supernovae on the Dynamical Evolution of Binary Stars and Star Clusters". In: *Handbook of Supernovae*. Ed. by Athem W. Alsabti and Paul Murdin. Cham: Springer International Publishing, pp. 2313–2329. ISBN: 978-3-319-21846-5. DOI: 10.1007/978-3-319-21846-5_116. URL: https://doi.org/10.1007/978-3-319-21846-5_116.

Pols, Onno (2011). *Stellar Structure and Evolution (Lecture Notes)*.

Postnov, Konstantin A. and Lev R. Yungelson (May 2014). "The Evolution of Compact Binary Star Systems". In: *Living Reviews in Relativity* 17.1, 3, p. 3. DOI: 10.12942/lrr-2014-3. arXiv: 1403.4754 [astro-ph.HE].

Prialnik, Dina (2009). *An Introduction to the Theory of Stellar Structure and Evolution*.

Sana, H. et al. (July 2012). "Binary Interaction Dominates the Evolution of Massive Stars". In: *Science* 337.6093, p. 444. DOI: 10.1126/science.1223344. arXiv: 1207.6397 [astro-ph.SR].

Smith, Nathan (Aug. 2014). "Mass Loss: Its Effect on the Evolution and Fate of High-Mass Stars". In: *ARA&A* 52, pp. 487–528. DOI: 10.1146/annurev-astro-081913-040025. arXiv: 1402.1237 [astro-ph.SR].

Soberman, G. E., E. S. Phinney, and E. P. J. van den Heuvel (Nov. 1997). "Stability criteria for mass transfer in binary stellar evolution." In: *A&A* 327, pp. 620–635. arXiv: astro-ph/9703016 [astro-ph].

Tan et al. (Jan. 2014). "Massive Star Formation". In: *Protostars and Planets VI*. Ed. by Henrik Beuther et al., p. 149. DOI: 10.2458/azu_uapress_9780816531240-ch007. arXiv: 1402.0919 [astro-ph.GA].

Tauris, T. M. and R. J. Takens (Feb. 1998). "Runaway velocities of stellar components originating from disrupted binaries via asymmetric supernova explosions". In: *A&A* 330, pp. 1047–1059.

Tokovinin, Andrei and Maxwell Moe (Feb. 2020). "Formation of close binaries by disc fragmentation and migration, and its statistical modelling". In: *MNRAS* 491.4, pp. 5158–5171. DOI: 10.1093/mnras/stz3299. arXiv: 1910.01522 [astro-ph.SR].

Tout, Christopher A. et al. (Nov. 1997). "Rapid binary star evolution for N-body simulations and population synthesis". In: *MNRAS* 291.4, pp. 732–748. DOI: 10.1093/mnras/291.4.732.

van Loon, J. Th. (May 2013). "Betelgeuse and the Red Supergiants". In: *EAS Publications Series*. Ed. by P. Kervella, T. Le Bertre, and G. Perrin. Vol. 60. EAS Publications Series, pp. 307–316. DOI: 10.1051/eas/1360036. arXiv: 1303.0321 [astro-ph.SR].

Villaume, Alexa et al. (Nov. 2017). "Initial Mass Function Variability (or Not) among Low-velocity Dispersion, Compact Stellar Systems". In: *ApJ* 850.1, L14, p. L14. DOI: 10.3847/2041-8213/aa970f. arXiv: 1710.11144 [astro-ph.GA].

Vink, Jorick S. (Sept. 2017). "Mass loss and stellar superwinds". In: *Philosophical Transactions of the Royal Society of London Series A* 375.2105, 20160269, p. 20160269. DOI: 10.1098/rsta.2016.0269. arXiv: 1610.00578 [astro-ph.SR].

Acknowledgements

I wish to thank my supervisor Ross Church for his infinite patience and understanding, his excellent advice and words of encouragement. Thanks also to David Hobbs for his support and flexibility. A very special thanks to Johan Rathsman for pulling me out of the fire. Thank you to my girls for putting up with me these last few years.

Appendix A

The aforementioned self-penned *Python* code, *HR.py*, as well as the additional snippets for supernovae simulations and data analysis can be accessed at https://vsredshift.github.io/HR/.